Cell

An HNF4α-miRNA Inflammatory Feedback Circuit Regulates Hepatocellular Oncogenesis

Maria Hatziapostolou,[1,2] Christos Polytarchou,[1,2] Eleni Aggelidou,[4] Alexandra Drakaki,[5] George A. Poultsides,[6] Savina A. Jaeger,[7] Hisanobu Ogata,[8] Michael Karin,[8] Kevin Struhl,[3] Margarita Hadzopoulou-Cladaras,[4,9] and Dimitrios Iliopoulos[1,2,9,*]

[1]Department of Cancer Immunology and AIDS, Dana-Farber Cancer Institute
[2]Department of Microbiology and Immunobiology
[3]Department of Biological Chemistry and Molecular Pharmacology
Harvard Medical School, Boston, MA 02115, USA
[4]Department of Genetics, Developmental and Molecular Biology, Laboratory of Developmental Biology, School of Biology, Aristotle University of Thessaloniki, Thessaloniki 54124, Greece
[5]Division of Hematology/Oncology, Department of Medicine, Beth Israel Deaconess Medical Center, Boston, MA 02215, USA
[6]Department of Surgery, Stanford University Medical Center, Stanford, CA 94305, USA
[7]Department of Developmental Molecular Pathways, Novartis Institute for Biomedical Research, Cambridge, MA 02139, USA
[8]Laboratory of Gene Regulation and Signal Transduction, School of Medicine, University of California, San Diego, La Jolla, CA 92093, USA
[9]These authors contributed equally to this work
*Correspondence: dimitrios_iliopoulos@dfci.harvard.edu
DOI 10.1016/j.cell.2011.10.043

SUMMARY

Hepatocyte nuclear factor 4α (HNF4α) is essential for liver development and hepatocyte function. Here, we show that transient inhibition of HNF4α initiates hepatocellular transformation through a microRNA-inflammatory feedback loop circuit consisting of miR-124, IL6R, STAT3, miR-24, and miR-629. Moreover, we show that, once this circuit is activated, it maintains suppression of HNF4α and sustains oncogenesis. Systemic administration of miR-124, which modulates inflammatory signaling, prevents and suppresses hepatocellular carcinogenesis by inducing tumor-specific apoptosis without toxic side effects. As we also show that this HNF4α circuit is perturbed in human hepatocellular carcinomas, our data raise the possibility that manipulation of this microRNA feedback-inflammatory loop has therapeutic potential for treating liver cancer.

INTRODUCTION

Hepatocellular carcinoma (HCC) is the main type of liver cancer and the third most common cause of cancer mortality worldwide. The major risk factor for HCC is chronic hepatitis, due to hepatotropic viruses (HBV, HCV) (El-Serag and Rudolph, 2007), but the molecular mechanisms leading to HCC have not been well characterized. Hepatocellular carcinogenesis involves many genetic and epigenetic alterations and is influenced by environmental factors. Genes such as c-*myc*, cyclin D1, p53, p16, E-cadherin, and PTEN have been linked to hepatocarcinogenesis (Villanueva et al., 2007). Persistent inflammation also impacts the course of liver tumor development (Coussens and Werb, 2002), and chronic inflammatory stimuli and increased STAT3 activation recapitulate hepatic oncogenesis in various animal models (He et al., 2010). In addition, the inflammatory responses induced by obesity or administration of the diethylnitrosamine (DEN) are known to promote HCC in mice (Park et al., 2010; Maeda et al., 2005).

HNF4α is a member of the nuclear receptor superfamily of ligand-dependent transcription factors (NR2A1) that is enriched in liver tissue (Zhong et al., 1993). HNF4α is indispensable for development and maintenance of the hepatic epithelium (Parviz et al., 2003) and also has links to a variety of human diseases, including diabetes, colitis, and cancer. A number of mutations within the HNF4A gene are considered to contribute to several forms of maturity-onset diabetes in children (Gupta and Kaestner, 2004). Suggesting a potential link between HNF4α and inflammation, genome-wide association studies have identified HNF4A as a susceptibility locus for ulcerative colitis (Barrett et al., 2009), and recent evidence supports an oncogenic role for HNF4α in intestinal cancer (Darsigny et al., 2010). But conflicting reports have assigned HNF4α both tumor-promoting and tumor-suppressing roles in liver cancer (Xu et al., 2001; Yin et al., 2008).

Here, we show that HNF4α is a key regulator of hepatocellular carcinogenesis. During hepatocellular transformation, transient inhibition of HNF4α becomes a stable event, with a feedback loop consisting of miR-124, IL6R, STAT3, miR-24, and miR-629 maintaining the hepatocyte-transformed phenotype in vitro and in vivo. Perturbation of this network, through miR-124 systemic administration, prevents and suppresses HCC development in a murine liver cancer model. Components of the HNF4α feedback loop circuit are differentially expressed in

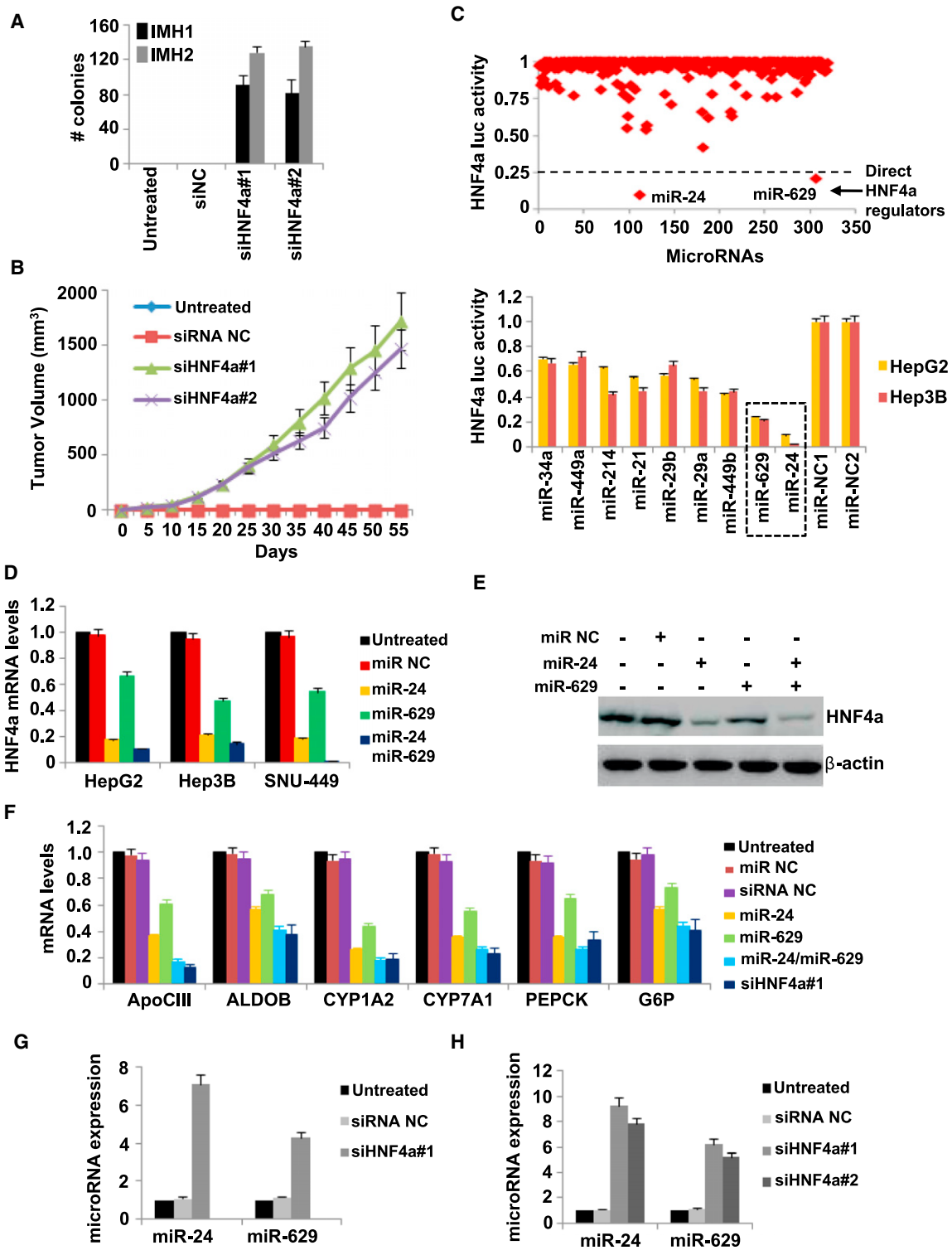

Figure 1. HNF4α Suppression through miR-24 and miR-629 Induces Hepatocellular Transformation

(A) Soft agar colony assay of nontransformed immortalized hepatocytes (IMH1, IMH2) treated for 48 hr with siRNA-negative control (siNC) or two different siRNAs against HNF4α (siHNF4α#1, siHNF4α#2). Colonies (mean ± SD) 50 μm were counted using a microscope 20 days later.

(B) Tumor volume (mean ± SD) in mice injected with IMH1 cells untreated or treated for 48 hr with siRNA NC, siHNF4α#1, or siHNF4α#2.

(C) Effects of microRNAs (primary screen) on HNF4α luciferase activity in HepG2 cells (top). The top nine hits identified from the primary microRNA library screen were tested in secondary screen in HepG2 and Hep3B cells (bottom).

human hepatocellular carcinomas relative to normal liver tissues. Though the epigenetic switch described here resembles an epigenetic switch that converts a nontransformed breast cell line into a stably transformed line that relies on an inflammatory feedback look involving STAT3 (Iliopoulos et al., 2009, 2010), the microRNA, transcription factors, and target genes mediating these epigenetic switches differ considerably in the breast and liver contexts. Overall, our data suggest that epigenetic switches are regulatory events that are essential for cancer initiation and maintenance in addition to mutational events.

RESULTS

Transient Inhibition of HNF4α Induces Hepatocellular Oncogenesis

To elucidate the role and function of HNF4α in liver cancer initiation, we modulated its expression in nontransformed immortalized human hepatocytes (IMH). We found that HNF4α inhibition transformed IMH cells and increased their invasiveness (Figures 1A and 1B and Figures S1A–S1C available online). Strikingly, transient inhibition of HNF4α was sufficient to induce transformation of IMH cells and promote tumor formation in immunodeficient mice (Figures 1A and 1B). In these tumors (day 55), HNF4α mRNA expression was still suppressed (Figure S1D), suggesting that inhibition of HNF4α initiates a feedback loop that continuously suppresses HNF4α expression and induces a stable transformed phenotype. In accordance with the data from our primary IMH cells, transient inhibition of HNF4α increased colony formation and invasiveness of HepG2 and SNU-449 cancer cells (Figures S1E and S1F) and decreased expression levels of HNF4a direct metabolic target genes (Figure S1G). Overall, these data suggest that HNF4α inhibition induces transformation of immortalized hepatocytes through a feedback regulatory mechanism.

miR-24 and miR-629 Suppress Directly HNF4α Expression during Hepatocellular Transformation

How is HNF4α suppression triggered and maintained during hepatocellular transformation? Recently, we and others have described the existence of dynamic microRNA-transcription factor networks in a variety of cancers (Iliopoulos et al., 2009, 2010; Kent et al., 2010). To identify microRNAs that regulate directly HNF4α expression, we performed a microRNA-based genetic screen (Figure 1C, top). MicroRNAs that inhibited HNF4α 3′UTR luciferase activity by more than 75% were scored as positive hits. These were further validated in HepG2 and Hep3B cells, seeded in 6-well plates, according to the same criteria (Figure 1C, bottom). Our approach resulted in the identification of two microRNAs, miR-24 and miR-629, as direct regulators of HNF4α expression.

Several lines of evidence indicate that miR-24 and miR-629 target HNF4α directly, binding to its 3′UTR. Sequence complementarity analysis revealed that HNF4α is a gene target of miR-24 and miR-629, and upon overexpression of miR-24 or miR-629, HNF4α mRNA levels are reduced 5-fold and 2-fold, respectively (Figure 1D). In addition, HNF4α protein levels drop (Figure 1E), and the direct downstream targets are downregulated by miR-24 and miR-629 (Figure 1F). In addition, combined expression of these two miRNAs resembles the effects of HNF4α knockdown (Figure 1F).

Transient inhibition of HNF4α by siRNA resulted in upregulation of both miR-24 and miR-629 in IMH cells (Figure 1G). We also identified increased expression of miR-24 and miR-629 in tumors derived from IMH cells treated with two different siRNAs against HNF4α (Figure 1H). Taken together, these data suggest that both microRNAs regulate directly HNF4α expression and are part of the feedback loop circuit.

miR-24 and miR-629 Play a Key Role in Hepatocellular Cancer Initiation and Growth

To assess the functional role of miR-24 and miR-629 in tumorigenicity, we tested whether their overexpression can transform two distinct immortalized hepatocyte cell lines. Expression of miR-24 and/or miR-629 is sufficient for hepatocellular transformation and colony formation in soft agar (Figure 2A). Though miR-24 has a stronger effect than miR-629, the combination of the two microRNAs closely resembles HNF4α knockdown. The ability of miR-24 or miR-629 to induce transformation in vitro led us to extend our results and examine their ability to regulate tumor initiation in vivo. Overexpression of miR-24 or miR-629, to a lesser extent, was sufficient for the induction of tumor initiation and growth (Figure 2B). These observations indicate that transient expression of either miR-24 or miR-629 is sufficient to induce stable transformation of hepatocytes in vitro and in vivo. Reduced HNF4α expression in miR-24/miR-629-treated tumors (Figure 2C) also indicates that both microRNAs cooperatively suppress HNF4α expression inducing a stable transformed state.

To address the functional role of miR-24 and miR-629 in the maintenance of the transformed phenotype, we tested the effects of their upregulation on the tumorigenicity of hepatocellular cancer cells. Overexpression of miR-24 or miR-629 in HepG2 and SNU-449 cells increased their ability to form colonies (Figure 2D) and their invasive capacity (Figure 2E). As expected, a combination of the two microRNAs exhibited the same effects with HNF4α inhibition. To delineate the role of miR-24 and miR-629 in HCC growth in vivo, we performed xenograft experiments

(D) HNF4α mRNA levels (mean ± SD of three independent experiments) assessed by real-time RT-PCR analysis in HepG2, Hep3B, and SNU-449 cells untreated or treated with 100 nM miR NC or miR-24 and/or miR-629 for 48 hr.

(E) HNF4α protein levels in HepG2 cells untreated or treated with 100 nM miR NC or miR-24 and/or miR-629 for 48 hr.

(F) mRNA levels of HNF4α direct targets (mean ± SD of three independent experiments) assessed by real-time RT-PCR analysis in HepG2 cells untreated or treated with 100 nM miR NC or miR-24 and/or miR-629 or siRNA NC or siRNA or siHNF4α#1 for 48 hr.

(G) miR-24 and miR-629 expression levels (mean ± SD of three independent experiments) assessed by real-time RT-PCR analysis in IMH1 cells that were untreated or treated for 48 hr with siRNA NC or siHNF4α#1.

(H) miR-24 and miR-629 expression levels (mean ± SD of three independent experiments) assessed by real-time RT-PCR analysis in tumors derived from injected IMH1 cells that were untreated or treated for 48 hr with siRNA NC or siHNF4α#1 or siHNF4α#2.

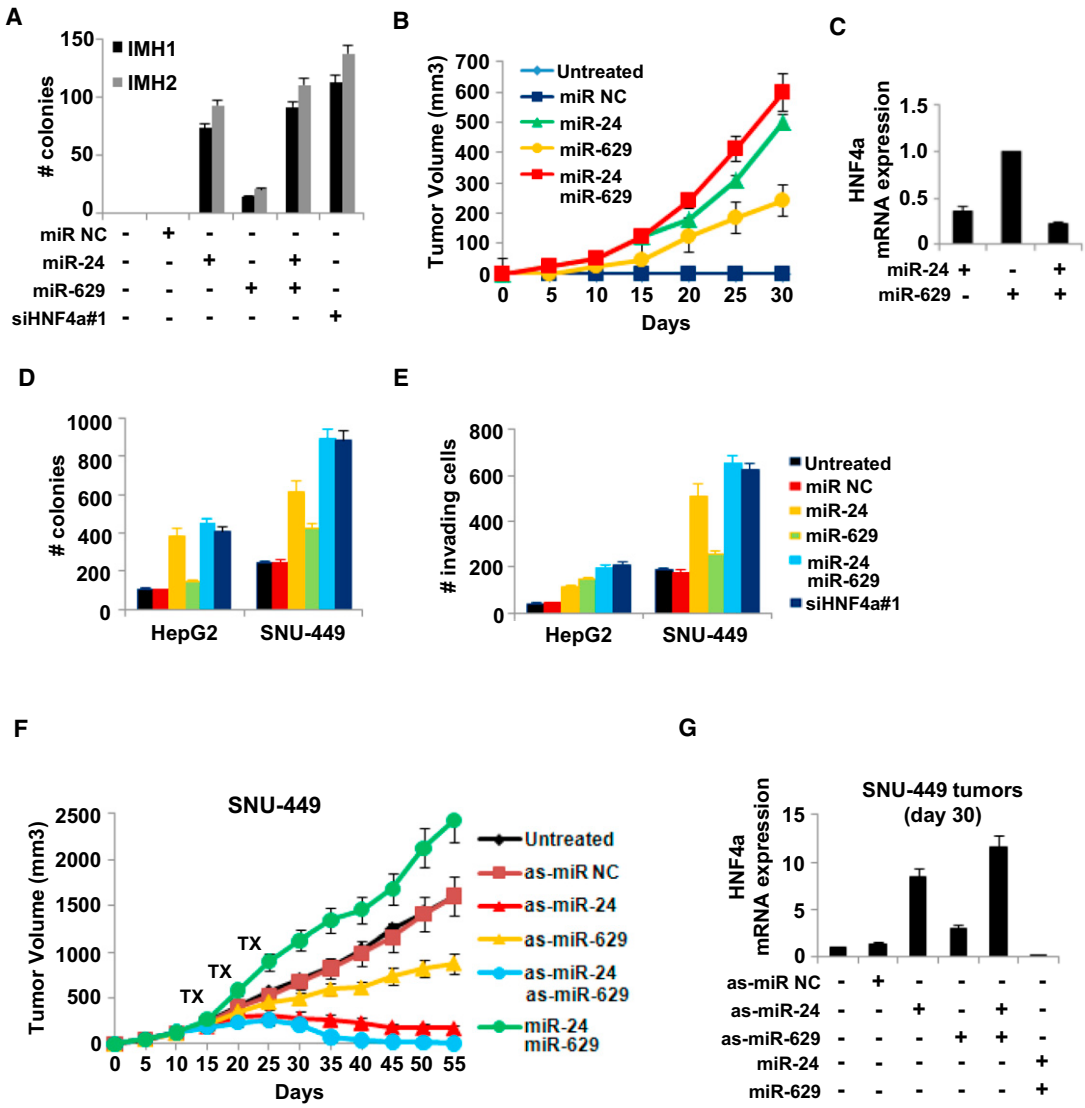

Figure 2. miR-24 and miR-629 Regulate the Induction and Stability of the Hepatocellular Transformed Phenotype

(A) Number of colonies (>50 μm) (mean ± SD) of IMH1 and IMH2 cells treated with 100 nM miR NC, miR-24, and/or miR-629 or siHNF4α#1 for 48 hr.

(B) Tumor volume (mean ± SD) in mice injected with IMH1 cells untreated or treated for 48 hr with 100 nM miR NC or miR-24 and/or miR-629.

(C) HNF4α mRNA levels assessed by real-time RT-PCR analysis in tumors (day 30) derived from IMH1 cells untreated or treated for 48 hr with 100 nM miR-24 and/or miR-629.

(D) Soft agar colony assay (mean ± SD) and (E) invasion assay (mean ± SD) of HepG2 and SNU-449 cells treated with 100 nM miR NC, miR-24, miR-629, or siHNF4α#1 for 24 hr.

(F) Tumor volume (mean ± SD) in mice injected with SNU-449 cells and treated with as-miR NC or as-miR-24 and/or as-miR-629, or miR-24 and miR-629.

(G) HNF4α mRNA levels (mean ± SD) in tumors (day 30) derived from mice treated with as-miR NC or as-miR-24 and/or as-miR-629 or miR-24 and miR-629.

in which SNU-449 cells were injected subcutaneously in immunodeficient mice (Figure 2F). We found that overexpression of miR-24 and miR-629 increased the growth of SNU-449 xenograft tumors (Figure 2F), whereas simultaneous inhibition of both microRNAs completely suppressed tumor growth. Are the effects of miR-24 and miR-629 on tumor growth related to HNF4α expression? We tested HNF4α mRNA levels in xenograft tumors (day 30) from the same mice, as described above. Tumors treated with the antisense microRNAs are smaller, contain many apoptotic cells (Figure S2), and exhibit elevated HNF4α mRNA levels (Figure 2G).

STAT3 Is a Direct Regulator of miR-24 and miR-629 Expression

According to our data, both miR-24 and miR-629 directly suppress HNF4α expression, and they are activated by inhibition of HNF4α expression in hepatocytes as part of the feedback loop circuit. We found that miR-24 and miR-629 are coordinately

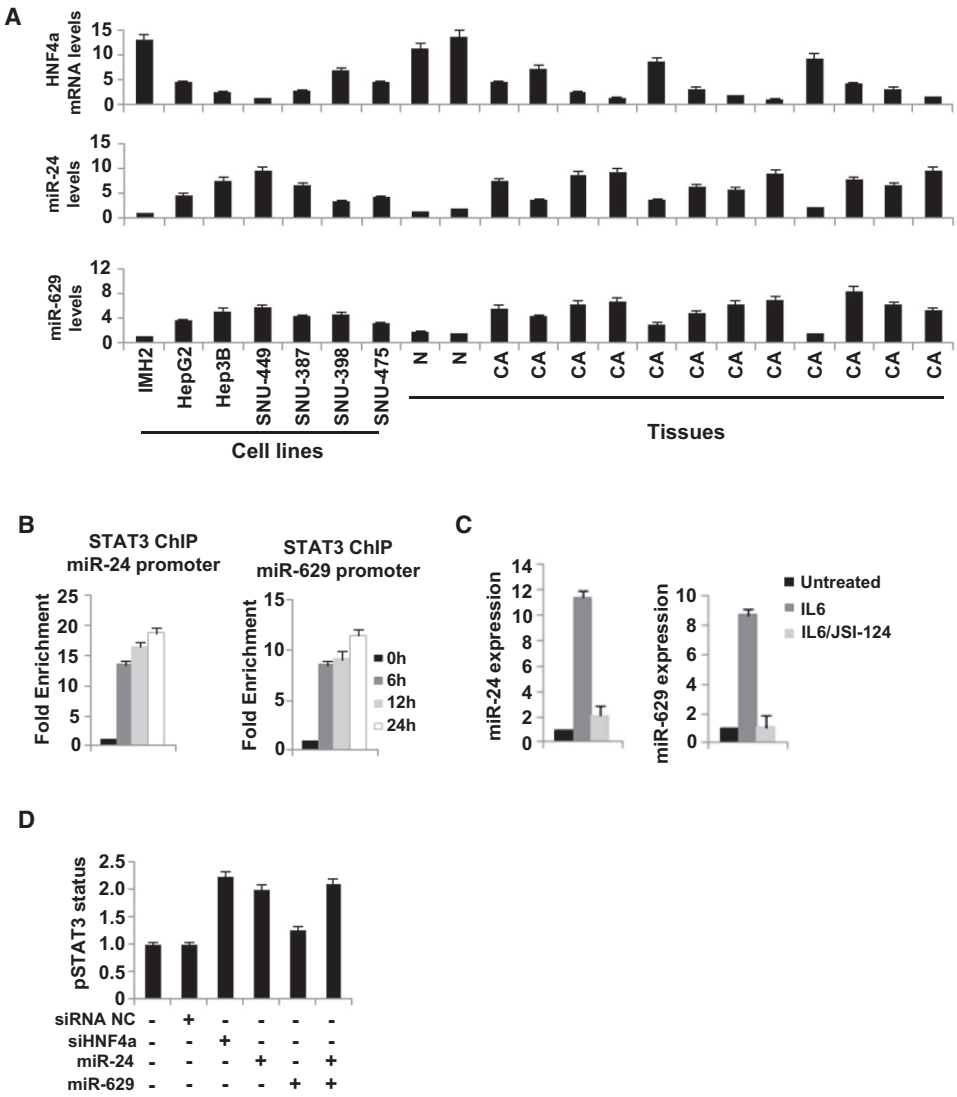

Figure 3. STAT3 Regulates miR-24 and miR-629 during Hepatocellular Transformation

(A) HNF4α, miR-24, and miR-629 levels (mean ± SD) in nontransformed immortalized hepatocytes (IMH2), different HCC lines, two normal liver tissues (N), and 12 hepatocellular cancer tissues (CA).

(B) STAT3 occupancy (fold enrichment) at the miR-24 and miR-629 loci, as determined by chromatin immunoprecipitation of crosslinked SNU-449 cells treated with IL6 (20 ng/ml) for 6, 12, or 24 hr.

(C) miR-24 and miR-629 expression levels (mean ± SD) in SNU-449 cells treated with IL6 (10 ng/ml) for 24 hr or JSI-124 (5 μg/ml) for 24 hr and then IL6 for 24 hr.

(D) STAT3 phosphorylation status (Tyr 705) assessed by ELISA in SNU-449 cells treated with 1 nM siRNA NC, siHNF4α#1, miR-24, and/or miR-629 for 24 hr. The data are presented as mean ± SD of three independent experiments.

upregulated in both hepatocellular cell lines and human tumors (Figure 3A). Examination of potential common transcription factor binding sites in miR-24 and miR-629 promoter areas revealed a highly conserved STAT3 binding motif in miR-24 promoter and a moderately conserved STAT3 motif in miR-629 promoter (Table S1). Chromatin immunoprecipitation (ChIP) analysis in SNU-449 cells revealed that, upon IL6 stimulation, STAT3 binds in miR-24 and miR-629 promoter regions, with binding to the highly conserved miR-24 site being stronger (Figure 3B). STAT3 activation by IL6 treatment resulted in upregulation of both miR-24 and miR-629 levels, whereas pharmacological inhibition of STAT3 (JSI-124) strongly reduced miR-24 and miR-629 expression levels (Figure 3C).

To determine whether STAT3 is a member of the HNF4α feedback loop circuit, we measured STAT3 phosphorylation levels upon overexpression of miR-24 and/or miR-629 or inhibition of HNF4α in SNU-449 cells (Figure 3D). Strikingly, all treatments significantly induced STAT3 phosphorylation when compared to the negative control samples. In accordance with our data above, miR-24 had a more pronounced effect (compared to miR-629), similar to that of HNF4α knockdown and the combinatorial expression of the two microRNAs. These results strongly

suggest that these microRNAs, STAT3, and HNF4α are part of an inflammatory feedback loop and not simply downstream effectors of IL6.

miR-124 Is a Direct Downstream Effector of HNF4α Activity and Part of the Feedback Loop Network

Recent studies have identified microRNA-transcription factor feedback loops in cancer cells (Fabbri et al., 2011; Iliopoulos et al., 2010). To further unravel the mechanism by which inhibition of HNF4α expression induces hepatocellular transformation through a feedback loop, we looked for HNF4a-binding sites in miRNA promoters. Lever algorithm analysis revealed HNF4α-binding sites in eight microRNA promoter areas (Table S2). ChIP analysis showed that HNF4α binds strongly (15- to 25-fold enrichment) to miR-124 promoter in HepG2 and SNU-449 cells (Figure 4A), and inhibition of HNF4α expression resulted in significant reduction of miR-124 levels (~5-fold) (Figure 4B). Similarly, miR-124 expression is significantly inhibited upon the combined overexpression of miR-24 and miR-629, and this inhibition is comparable with the one caused by HNF4α knockdown. Based on our observation of an inverse correlation between STAT3 activation and HNF4α expression, we examined how IL6 treatment influenced activity of a luciferase reporter construct containing the miR-124 promoter (Figure 4C). Treatment of HepG2 cells with IL6 significantly inhibited the activity of the miR-124 luciferase reporter, whereas there was no effect when the HNF4α site was mutated.

As HNF4α directly regulates miR-124 expression in HCC lines, we tested the possibility that miR-124 may mediate the HNF4α-regulated inhibition of STAT3. Interestingly, STAT3 activation was induced upon miR-124 suppression when compared to the respective negative controls (Figure 4D). The above experiments suggest that miR-124 participates also in the HNF4α feedback loop. To further show that miR-124 is a member of this loop, we examined IMH1 transformation efficiency upon inhibition of miR-124 expression. As expected, inhibition of miR-124 expression strongly induces colony formation, and this effect is reversed by STAT3 knockdown or combined suppression of miR-24 expression (Figure 4E). Likewise, suppression of miR-124 or knockdown of HNF4α induces colony formation and invasiveness of HepG2 and SNU-449 cells, whereas overexpression of miR-124 in these cell lines reverses the phenotype (Figure S3). Taken together, these observations are consistent with a pathway in which STAT3 activation inhibits HNF4α expression, which leads to suppressed expression of miR-124 and establishes an inflammatory feedback loop that is necessary and sufficient for human hepatocyte transformation.

miR-124 Targets IL6R and Consequently Modulates IL6R/STAT3 Pathway during Hepatocellular Transformation

Because STAT3 activation is suppressed by miR-124, we hypothesized that miR-124 might target one of the components of the IL6-STAT3 pathway. In support of this hypothesis, sequence complementarity and conservation analysis revealed that interleukin 6 receptor (IL6R) is a potential direct gene target of miR-124. Furthermore, miR-124 and IL6R expression levels are inversely correlated in IMH1 cells and five hepatocellular cancer cell lines (Figure 4F). In addition, suppression of miR-124 expression, either directly by antisense miR-124 or indirectly by knockdown of HNF4α, leads to induced expression of IL6R (Figure 4G). Conversely, overexpression of miR-124 significantly reduced IL6R mRNA and protein levels (Figures 4G and 4H). Also, miR-124 overexpression inhibits the activity of a luciferase reporter construct containing the IL6R 3′UTR and vice versa (Figure 4I). Next, phosphorylation of STAT3, a downstream target of IL6R, is induced by inhibition of miR-124 expression or knockdown of HNF4α (Figure 4J). In addition to IL6R, we found that inhibition of miR-124 expression results in increased IL6 production (Figure S4A), suggesting that miR-124 regulates STAT3 activity by affecting the IL6-IL6R levels and pathway. Similar effects were identified when HNF4α was suppressed. Specifically, HNF4α inhibition resulted in increased levels of soluble IL6 and IL6R (Figures S4B and S4C), which, in turn, increased liver tumorigenicity (Figure S4D). These experiments support a central role for HNF4α in regulating the IL6-STAT3 inflammatory response.

The Feedback Loop Involving HNF4α, miR-124, IL6R, STAT3, miR-24, and miR-629 Is Required for the Induction and Maintenance of the Transformed Phenotype in Hepatocytes

To examine the dynamics of this circuit during the transformation of hepatocytes, IMH1 cells were transiently transfected with the respective microRNAs or siRNAs and 96–480 hr posttransfection were plated in soft agar and injected in mice (Figures S5A and S5B). Suppression of miR-124 or HNF4α or overexpression of miR-24 or miR-629 induced hepatocellular transformation. We also find that the kinetics of STAT3 activation along with expression levels of miR-124, miR-24, miR-629, and HNF4α demonstrate the establishment and maintenance of the regulatory loop even 480 hr after transfection (Figures S5C–S5G). In addition to transcriptional activation, we show that suppression of HNF4α led to increased soluble IL6 and IL6R levels (Figure S5H), hepatocyte hyperproliferation, and decreased apoptosis (Figure S6). On the other hand, breaking the regulatory circuit by manipulation of different members of the loop blocked the stable transformed phenotype of human hepatocytes (Figures S5I and S5J). Overall, these data indicate that HNF4α is a central regulator of hepatocyte growth and transformation.

HNF4α-miRNA Inflammatory Circuit Is Perturbed during HCC Development in Mice

Building on our in vitro findings, we asked whether the HNF4α circuit is perturbed during development of chemical-induced hepatocellular carcinogenesis in vivo. To exclude the possibility that the IL6/STAT3 pathway is activated by Kupffer cells, we examined the expression levels of HNF4α, miR-124, IL6R, and miR-24 in purified hepatocytes derived from DEN-treated mice (Figure 5A). In accordance with our in vitro data, we identified that the HNF4α-miRNA circuit is perturbed in hepatocytes during HCC development in mice. Interestingly, HNF4α suppression started on week 4, whereas miR-24 was upregulated on week 24, when the tumors have already been formed. These data are consistent with the idea that early suppression of HNF4α

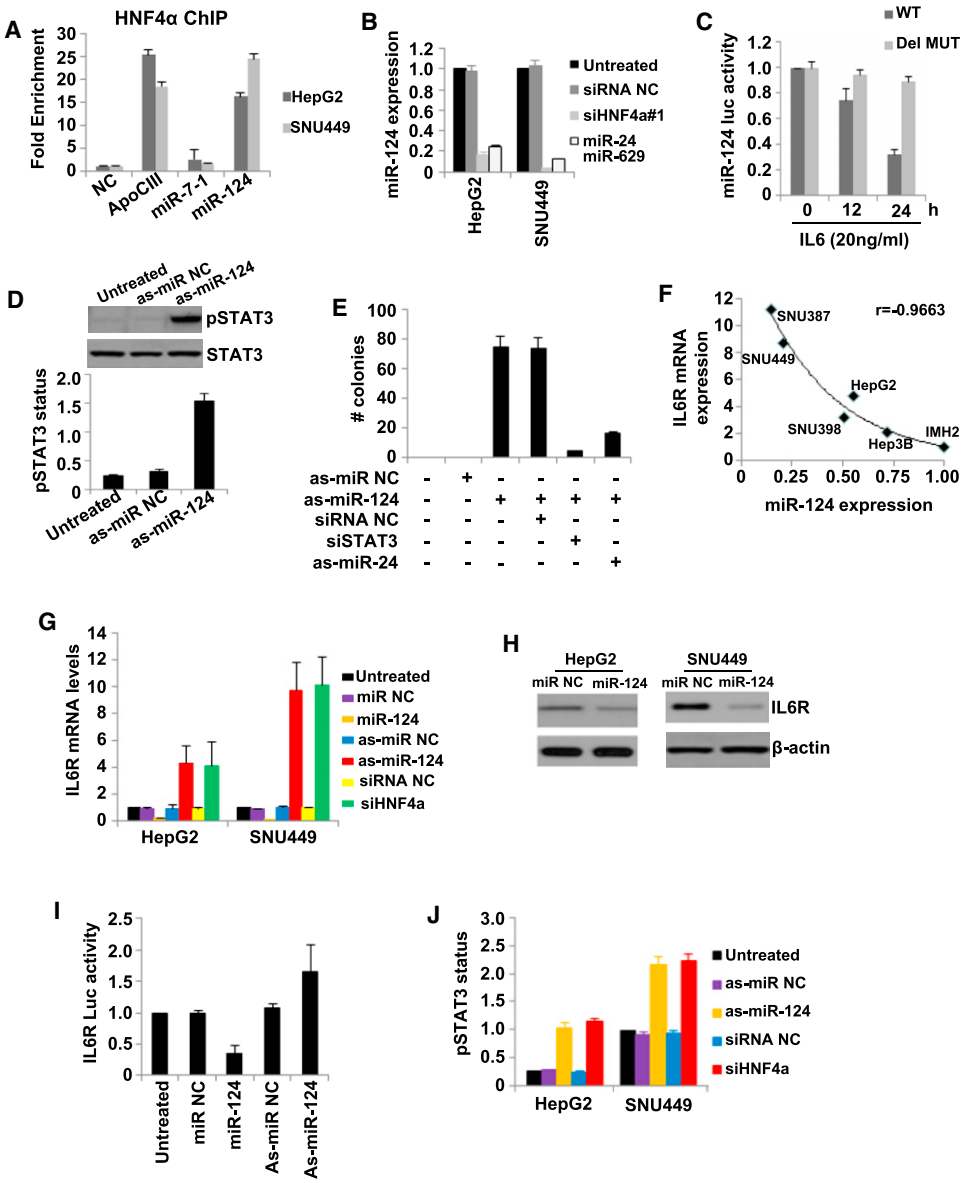

Figure 4. HNF4α Binds and Regulates miR-124, which Controls Directly IL6R Expression in Hepatocytes

(A) HNF4α occupancy (fold enrichment) (mean ± SD) in ApoCIII, miR-7-1, and miR-124 promoter areas.

(B) miR-124 levels (mean ± SD) in HepG2 and SNU-449 treated with siRNA NC, siHNF4α#1, miR-24, and miR-629 for 24 hr.

(C) Luciferase activity (mean ± SD) of a reporter construct harboring miR-124 promoter (wild-type or deletion mutant in the HNF4α-binding site) 12 and 24 hr posttreatment with IL6 (10 ng/ml) in HepG2 cells.

(D) STAT3 phosphorylation status (Tyr 705) (mean ± SD) evaluated by ELISA and western blot analyses after treatment with as-miR-NC or as-miR-124 for 24 hr in HepG2 cells.

(E) Number of colonies (mean ± SD) of nontransformed immortalized hepatocytes (IMH1) treated with as-miR NC or as-miR-124 together with siRNA NC or siRNA against STAT3 (siSTAT3) or as-miR-24 for 24 hr. The data are presented as mean ± SD of three independent experiments.

(F) miR-124 and IL6R levels in the indicated cell lines and a correlation coefficient (r) are shown.

(G) IL6R mRNA levels (mean ± SD) in HepG2 and SNU-449 cells treated for 24 hr with miR-NC, miR-124, as-miR NC, as-miR-124, siRNA NC, and siHNF4α.

(H) IL6R protein levels in HepG2 and SNU-449 cells treated for 24 hr with miR-NC or miR-124.

(I) Luciferase assay using a reporter construct containing the 3′UTR of IL6R, 24 hr after transfection with miR-NC, miR-124, as-miR NC, and as-miR-124. The data are presented as (mean ± SD).

(J) STAT3 phosphorylation status (Tyr 705) evaluated by ELISA in HepG2 and SNU-449 cells treated for 24 hr with as-miR NC, as-miR-124, siRNA NC, and siHNF4α. The data are presented as mean ± SD of three independent experiments.

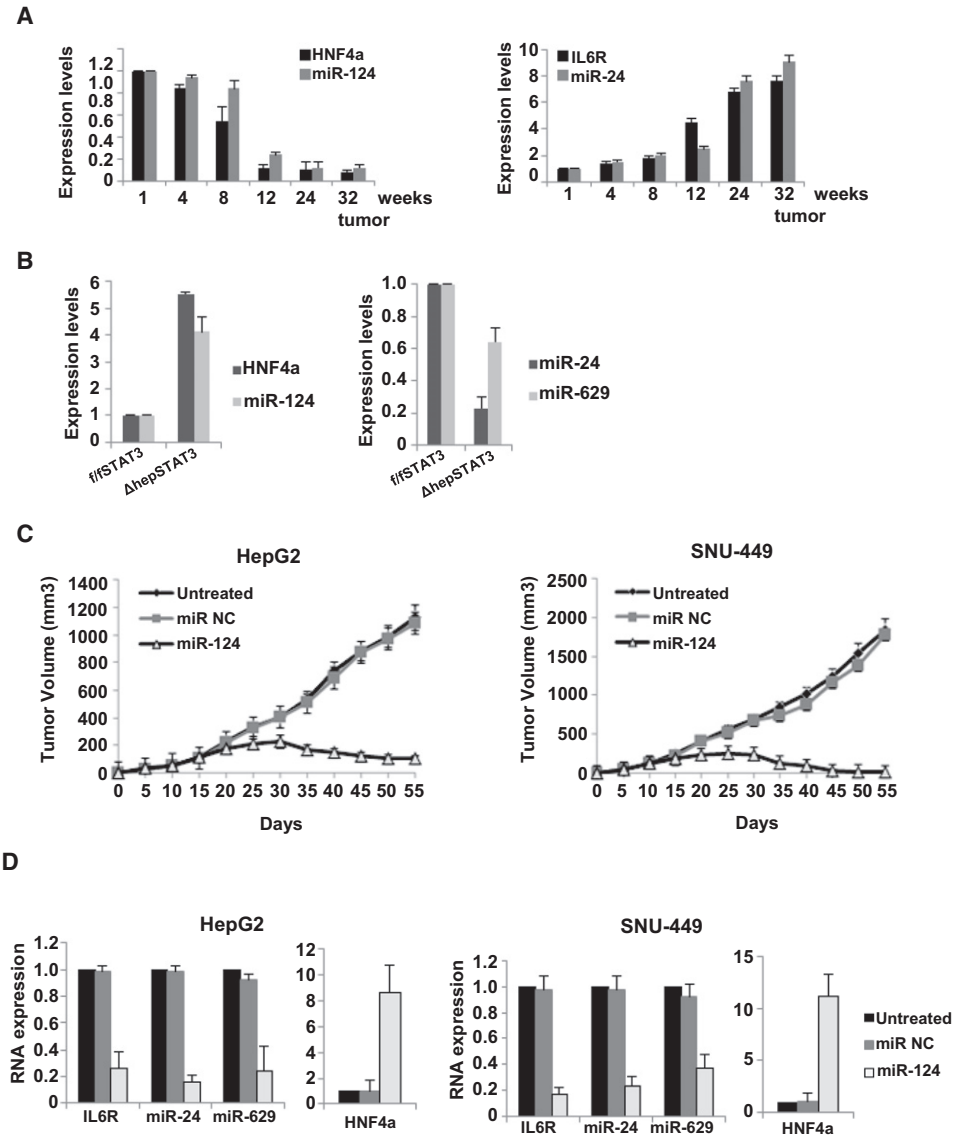

Figure 5. The HNF4α Circuit Is Perturbed during HCC Development

(A) Assessment of HNF4α, miR-124, IL6R, and miR-24 levels (mean ± SD) in purified hepatocytes during DEN-induced liver carcinogenesis in mice.

(B) Evaluation of HNF4α mRNA levels and miR-124, miR-24, and miR-629 levels derived from DEN-treated male $STAT3^{f/f}$ and $STAT3^{\Delta hep}$ mice. The experiments have been performed in triplicate, and data show mean ± SD.

(C) Tumor volume (mean ± SD) in mice injected with HepG2 and SNU-449 cells treated with miR NC or miR-124. Treatments were repeated every 5 days, and tumor volume was monitored every 5 days for 55 days.

(D) IL6R, miR-24, miR-629, and HNF4α levels (mean ± SD) assessed by real-time RT-PCR analysis, in tumors (day 30) derived from mice treated with miR NC or miR-124.

leads to activation of the miRNA inflammatory circuit during HCC development.

In addition, we tested whether the HNF4α-miRNA circuit is perturbed in hepatocyte-specific STAT3-deficient mice ($STAT3^{f/f}$/Alb-Cre = $STAT3^{\Delta hep}$). It is known that the DEN-treated $STAT3^{\Delta hep}$ mice develop fewer and much smaller tumors in comparison to the DEN-treated $STAT3^{f/f}$ mice (He et al., 2010). Consistent with our hypothesis, we identified that tumors derived from DEN-treated $STAT3^{\Delta hep}$ mice had increased HNF4α and miR-124 levels and decreased miR-24 and miR-629 levels in comparison to DEN-treated $STAT3^{f/f}$ mice (Figure 5B). These data show that suppression of the inflammatory response in vivo perturbs the HNF4α circuit, suggesting that this circuit can be affected at any step.

Perturbation of the HNF4α Circuit Has Therapeutic and Preventive Effects in Different Murine Liver Cancer Models

To further validate the in vivo significance of the HNF4α circuit, we asked how perturbation of this circuit would affect tumor growth

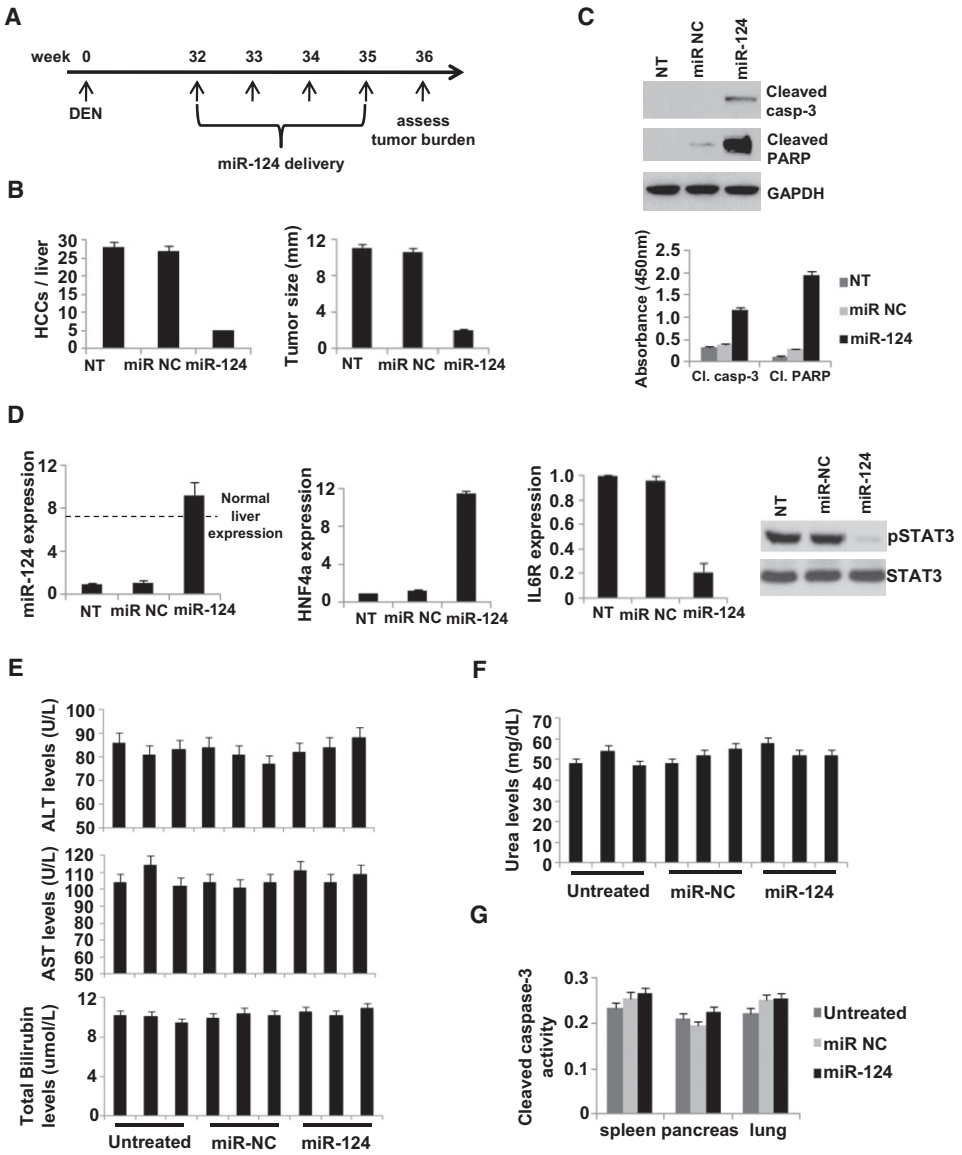

Figure 6. Modulation of the HNF4α Circuit Prevents and Suppresses HCC Development in Mice

(A) Timeline of miR-124 therapeutic delivery experiment.

(B) Number of HCC tumors/liver and tumor size (mm^3) (mean ± SD) in nontreated (NT), miR-NC-, and miR-124-treated mice (week 36).

(C) Levels of cleaved PARP and caspase-3 in untreated, miR NC-, and miR-124-treated mice (week 36) assessed by ELISA and western blot analyses.

(D) Evaluation of miR-124 levels, HNF4α levels, and IL6R levels by real-time PCR and STAT3 phosphorylation status (Tyr705) by western blot in tumors derived from nontreated (NT), miR-NC-, and miR-124-treated mice (week 36). The data are shown as mean ± SD.

(E and F) Levels of (E) alanine aminotransferase (ALT), aspartate aminotransferase (AST), total bilirubin, and (F) urea were assessed in the serum of mice treated with 10 mg/kg miR-NC or miR-124 for 48 hr. Each bar represents a different mouse. The experiment was performed in triplicate, and the data show mean ± SD.

(G) Cleaved caspase-3 activity (mean ± SD) assessed by ELISA assays in tissues (spleen, pancreas, heart) derived from untreated, miR-NC-, or miR-124-treated mice.

in different HCC mouse models. Specifically, the inhibitory role of miR-124 on hepatocellular neoplastic transformation suggested the possibility that HCC-derived tumors could be eradicated efficiently by interference with the feedback loop on the level of miR-124. We found that miR-124 treatment suppressed HepG2 and SNU-449 xenograft tumor growth (Figure 5C) by reducing IL6R, miR-24, and miR-629 expression levels and significantly increasing HNF4α expression (Figure 5D).

In addition to the subcutaneous HCC mouse model, we tested whether systemic administration of miR-124 is able to suppress HCC tumor growth in DEN-treated mice. According to our treatment protocol, miR-NC or miR-124 was systemically administered in DEN-treated mice on a weekly basis (first day of the week) for four cycles (weeks 32, 33, 34, and 35) (Figure 6A). On week 36, the mice were sacrificed, and we assessed the tumor burden. We found that miR-124 suppressed > 80% HCC tumor

growth and size (Figure 6B) through induction of apoptosis (Figure 6C), and actually, miR-124 administration resulted in restoration of physiological miR-124 expression, whereas miR-NC administration did not have any effect (Figure 6D). In addition, miR-124 delivery perturbed the HNF4α circuit through upregulation of HNF4α mRNA levels, IL6R suppression, and inhibition of STAT3 activation (phosphorylation). Importantly, we found that systemic delivery of miR-NC or miR-124 did not affect liver and kidney function (Figures 6E and 6F) and did not have any toxicity effects on essential organs (Figure 6G). These data demonstrate that miR-124 administration does not affect the physiology of mice through induction of cytotoxic effects.

In addition to therapeutic effects, we examined whether perturbation of the HNF4α circuit can prevent HCC development in mice. We identified that miR-124 delivery restored the physiological levels of this microRNA in liver tumors, even 2 weeks postinjection (Figure S7A). According to these data, miR-124 was administered systemically on week 12 every 2 weeks until week 30, and at week 32, we assessed tumor burden (Figure S7B). We found that miR-124 delivery prevented efficiently HCC tumor growth in DEN-treated mice (Figure S7C), suggesting that the HNF4α-miRNA inflammatory circuit is essential for HCC development in vivo.

The HNF4α Regulatory Circuit Is Perturbed in Human HCC Tissues

We examined the expression levels of miR-24, IL6R, miR-124, and HNF4α in total RNA extracted from 12 normal liver tissues and 45 hepatocellular carcinomas (HCCs). We found that HNF4α and miR-124 were downregulated, whereas miR-24 and IL6R mRNA levels were increased in liver cancers relative to normal tissues (Figure 7A). In addition, immunohistochemical (IHC) analysis for HNF4α and phosphorylated STAT3 and in situ hybridization for miR-124, miR-24, and miR-629 revealed that, in 13/30 (43.3%) of HCC tumors, the circuit is perturbed (Figure 7B).

Due to the fact that our in vitro data suggest that activation of an inflammatory response through suppression of HNF4α levels is cell autonomous, we examined the activation of the inflammatory circuit in the absence of Kupffer cells. We tested expression levels of each member of the HNF4α circuit in RNA samples derived from laser capture microdissected hepatocytes, which were negative for CD45 expression. Specifically, in all (8/8) human normal liver tissues, we found high HNF4α and miR-124 levels and low IL6R, miR-24, and miR-629 levels. On the other hand, we identified that the HNF4α circuit is perturbed (HNF4α and miR-124 low levels; IL6R, miR-24, and miR-629) in 18/31 of human hepatocellular carcinomas (Figure 7C). Furthermore, in the same samples, we tested whether there is any correlation between the RNA expression levels of the different members of this circuit. We found an inverse correlation between HNF4α and miR-24 or miR-629 levels, an inverse correlation between miR-124 and IL6R levels, and a positive correlation between HNF4α and miR-124 levels (Figure 7D). Also, in the same human tissue samples, we examined IL6 and IL6R protein levels and STAT3 phosphorylation status and identified that the HCC samples (n = 18) with perturbed HNF4α circuit have higher levels in comparison to the HCC samples (n = 13) with nonperturbed HNF4α circuit or normal liver tissues (n = 8) (Figure 7E).

Furthermore, we were interested in identifying whether the HNF4α circuit is perturbed not only during liver cancer initiation, but also during liver cancer progression. Thus, we examined the mRNA expression levels of the different members of the circuit in different stages of HCC oncogenesis. We found that HNF4α and miR-124 levels were decreased, whereas IL6R and miR-24 levels were increased, during HCC progression (Figure 8A). Interestingly, the activity of this circuit correlated to HCC grade (Figure 8B). Overall, these data strongly suggest that, in addition to tumor initiation, the HNF4α-miRNA inflammatory feedback circuit is important for the progression of human cancer.

DISCUSSION

An HNF4α Circuit Is Essential for the Transformation of Immortalized Hepatocytes

Our data reveal the dynamics of a complex molecular self-reinforcing circuit that involves HNF4α, miR-124, IL6R, STAT3, and miR-24/miR-629 in the regulation of hepatocellular transformation and liver cancer (Figure 7F). The first component of the circuit links HNF4α to STAT3 activation, with HNF4α controlling IL6R expression through transcriptional regulation of miR-124. Although miR-124 has been identified as a cancer-associated tumor suppressive microRNA (Lujambio et al., 2007), its regulation and mode of action has been elusive. Here, we show that HNF4α binding and transcriptional regulation of miR-124 are comparable to the bona fide HNF4α target ApoCIII (Kardassis et al., 1997; Ladias et al., 1992). The second component of the circuit connects STAT3 activity to HNF4α expression via regulation of miR-24 and miR-629. Perturbations of the STAT3-HNF4α axis interfere with processes that govern hepatic transformation and oncogenesis, mechanistically linking inflammation and liver cancer.

An Epigenetic Switch Regulates Hepatocyte Transformation

The main characteristic of the HNF4α feedback circuit is that it transforms immortalized human hepatocytes by converting a transient signal (e.g., acute HNF4α inhibition) into a stable signal. Overexpression of any positive factor (miR-24, miR-629) or inhibition of any negative factor (HNF4α, miR-124) transforms immortalized hepatocytes, indicating that the loop can be affected at any step. Thus, the initiating event in different HCC mouse models and patients can be different. It is not necessary that the loop begins with reduction of HNF4α. According to our data, suppression of HNF4α expression is the first event in DEN-treated mice, followed by perturbation of the other members of the loop. In other scenarios, the IL6-STAT3 axis may activate the loop by different extracellular stimuli. Specifically, secreted IL6 from different immune cells in the tumor microenvironment, including Kupffer cells, could initiate this axis. For example, recent studies show that IL-22, a cytokine secreted by Th17 cells, controls hepatocellular oncogenesis via upregulation of STAT3 activity (Jiang et al., 2011), and hepatitis C viral infection can promote STAT3 activation (Tacke et al., 2011). Interestingly, miR-124 has been found epigenetically

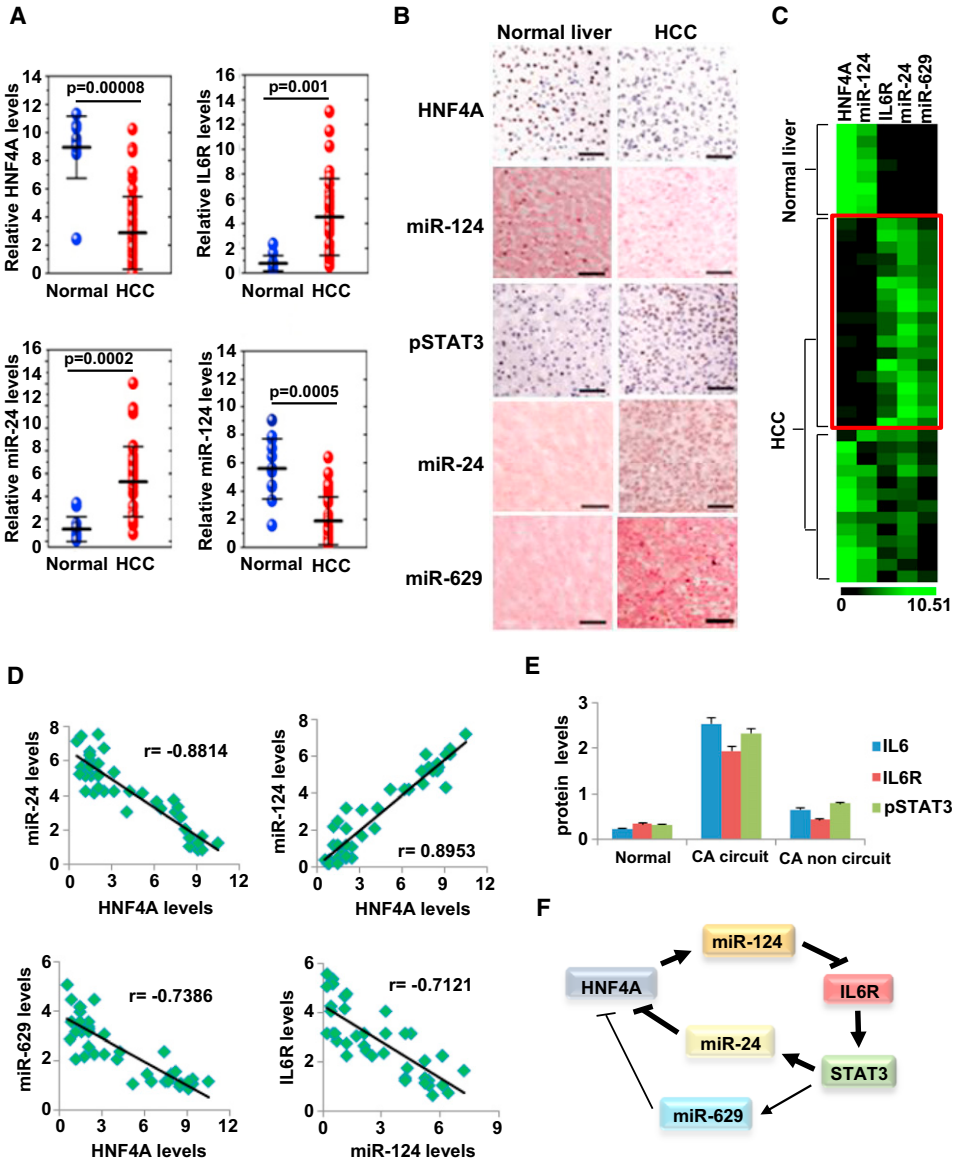

Figure 7. HNF4α Circuit Is Perturbed in Human Hepatocellular Carcinomas

(A) Assessment of HNF4α, IL6R, miR-24, and miR-124 levels (mean ± SD) by real-time PCR analysis in total RNAs derived from 12 normal liver tissues and 45 hepatocellular carcinomas.

(B) Immunohistochemistry for HNF4α, pSTAT3, and in situ hybridization for miR-124 and miR-24 in FFPE sections of hepatocellular carcinomas and normal liver tissues. Sections were subjected to immunohistochemistry for HNF4α (DAB staining, brown) and phospho-STAT3 (Tyr705) (DAB staining) and counterstained with hematoxylin (blue) and in situ hybridization for miR-124, miR-24, and miR-629 and counterstained with nuclear fast red. Scale bar, 100 μm.

(C) Heatmap representation of HNF4α, IL6R, miR-24, and miR-124 levels assessed by real-time PCR (mean ± SD) in tissue-microdissected FFPE sections of eight normal liver tissues and 31 hepatocellular carcinomas.

(D) Correlation between the expression levels of different members of the HNF4α circuit (same samples as in Figure 7C). Each data point represents an individual liver tissue sample, and a correlation coefficient (r) is shown.

(E) Levels of IL6, IL6R, and pSTAT3 (Tyr705) assessed by ELISA in eight normal liver tissues, 31 hepatocellular carcinomas (18 tissues with activation of the HNF4α circuit [CA circuit] and 13 liver cancer tissues without activation of the HNF4α circuit [CA noncircuit]). The data are presented as mean ± SD of three independent experiments.

(F) Schematic representation of the proposed HNF4α feedback circuit in hepatocellular oncogenesis.

silenced through tumor-specific methylation both in human HCC cell lines and tissues (Furuta et al., 2010), and therefore miR-124 downregulation may be the first event that triggers hepatic carcinogenesis. Together, all of these data suggest that the initial event that activates this circuit could differ from patient to patient.

Due to the fact that the epigenetic switch in immortalized hepatocytes occurs within a few days, it is extremely unlikely

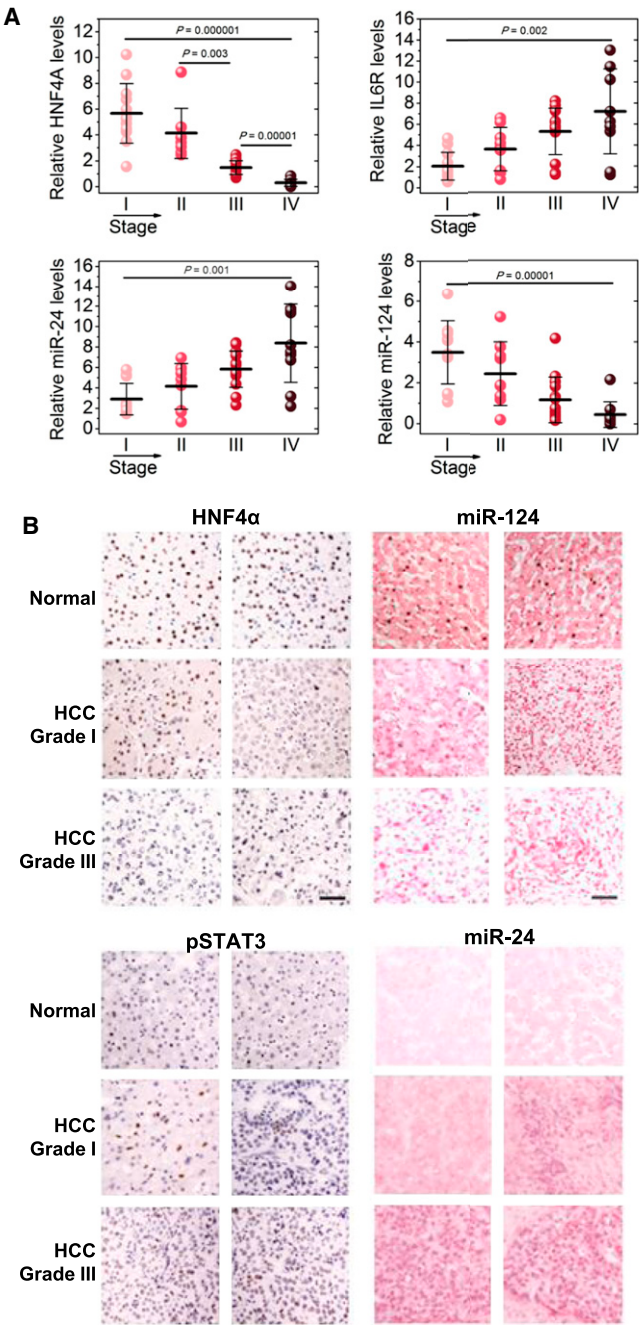

Figure 8. HNF4α Circuit Is Perturbed during HCC Progression

(A) Assessment of HNF4α, IL6R, miR-24, and miR-124 levels in total RNAs derived from 45 hepatocellular carcinomas, according to their tumor stage. The experiments have been performed in triplicate, and data are shown as mean ± SD.

(B) HCC sections were subjected to immunohistochemistry for HNF4α and phospho-STAT3 (Tyr705) (DAB staining, brown) and counterstained with hematoxylin (blue) and in situ hybridization for miR-124 and miR-24 and counterstained with nuclear fast red. Representative pictures are shown from normal, HCC grade I, and HCC grade III tissues.

Scale bar, 50 μm.

to involve changes in the DNA sequence, which is consistent with the definition of a true epigenetic switch (Ptashne, 2009). This notion of a self-reinforcing feedback loop that controls hepatocellular transformation comes in line with our previous observation of an epigenetic switch that mediated transformation of immortalized mammary epithelial (MCF10A) cells to a stably transformed cell (Iliopoulos et al., 2009, 2010). Furthermore, the identification of an epigenetic switch in hepatocellular transformation indicates that it is not a rare mechanism involved in cellular transformation and supports the possibility that cancer cells of diverse developmental origin might share a common mechanism for the establishment of the transformed state.

Our data also suggest that microRNA transcription factor regulatory circuits mediate epigenetic switches that induce transformation of immortalized cells. Recent reports posit that transcriptional (TFs) and nontranscriptional elements (microRNAs) may cooperate to tune gene expression in various biological processes (Chen et al., 1994; Gerstein et al., 2010; Martinez et al., 2008), including oncogenesis (Fabbri et al., 2011; Kent et al., 2010). Various network motifs have been proposed, but miRNA-TF feedforward and feedback loops predominate. For example, a feedforward regulatory circuit (KRAS-miR-143/miR-145) plays an essential role in pancreatic tumorigenesis (Kent et al., 2010). Taken together, these observations demonstrate that transcription factors participate in similar circuits that regulate induction and maintenance of stable transformation programs, suggesting that use of analogous regulatory loops may be a widespread property of oncogenic processes.

Role of HNF4α and Its Downstream Effectors in Hepatocellular Oncogenesis

HNF4α has long been considered a key transcription factor during liver embryonic development (Kyrmizi et al., 2006; Parviz et al., 2003). In the adult liver, HNF4α is expressed at high levels and binds to the promoter of 12% of genes expressed (Odom et al., 2004). Nevertheless, HNF4α's role in hepatocellular cancer and the mechanisms involved are far from clear. It has been shown that HNF4α is upregulated in human hepatocellular carcinoma (Xu et al., 2001) and, on the other hand, impedes the formation of liver tumors in mice by inducing differentiation of malignant cells—including cancer stem cells—into mature hepatocytes (Yin et al., 2008). Recent findings that the Wnt/β-catenin pathway interacts with HNF4α in intestinal epithelial cells (Cattin et al., 2009) and hepatocytes (Colletti et al., 2009) strengthen the notion that HNF4α acts as a tumor suppressor gene in both cancer types. Our study refines the repressive role of HNF4α in hepatic neoplasia, suggesting that HNF4α inhibition mediates an epigenetic switch that is essential for the transformation of immortalized hepatocytes.

Inflammation is one of the downstream mechanisms linking HNF4α to hepatocellular carcinogenesis. The protective action of HNF4α against inflammatory bowel diseases (Ahn et al., 2008; Darsigny et al., 2010) and the potential associations between the HNF4A locus and ulcerative colitis (Barrett et al., 2009) raise the possibility that this multifaceted transcription factor is a potent mediator of inflammatory responses (Marcil et al., 2010). Several studies have identified STAT3 as an oncogenic transcription factor activated by inflammatory responses

(Bromberg et al., 1999; Grivennikov et al., 2009; Iliopoulos et al., 2009; Iliopoulos et al., 2010), and IL6 is known to directly activate STAT3 (Zhong et al., 1994). STAT3 activity has been correlated with poor prognosis in HCC patients (Calvisi et al., 2006), and STAT3 inhibitors inhibit the growth of several human cancers (Hedvat et al., 2009), including HCC development and growth in mice (He et al., 2010).

As genetic alterations that result in constitutive STAT3 activation in hepatocytes only cause benign hepatic adenomas unless combined with oncogenic mutations (Rebouissou et al., 2009), it will be important to discover the parameters that distinguish primary hepatocytes from nontransformed immortalized cells. Although a transient inflammatory signal is insufficient to trigger such an epigenetic switch in normal hepatocytes, our in vivo data suggest that the epigenetic switch described here is relevant to human cancer. The epigenetic switch requires that a transient inflammatory response is converted to a chronic inflammatory response, with no resolution phase but continuous enhancement of the inflammatory signal. Thus, the results presented here provide a paradigm in which a key step in transformation involves an epigenetic switch in response to an inflammatory signal, as opposed to a mutational change in a tumor suppressor or oncogene. In support of this idea, recent data suggest that chronic activation of the IL6-STAT3 axis contributes to the transformation of hepatocytes that have acquired oncogenic mutations upon exposure to environmental and dietary carcinogens (Park et al., 2010).

Therapeutic and Preventive Effects of miR-124 Delivery in Hepatocellular Carcinogenesis

We show that miR-124 administration restored miR-124 expression to physiological levels in the liver, inhibiting and preventing DEN-induced hepatocellular carcinogenesis in mice. Previous studies have aimed to suppress microRNA expression in animal models through delivery of antagomirs or locked nucleic acid (LNA) oligomers (Elmén et al., 2008; Esau et al., 2006). Few studies have investigated the therapeutic delivery of microRNAs in vivo. A recent study has shown that restoration of miR-26a expression levels by an adeno-associated virus (AAV) suppresses liver tumorigenesis in liver-specific MYC transgenic mice (Kota et al., 2009) without any cytotoxic effects.

Our data suggest that systemic delivery of miR-124 may be a clinically viable anticancer therapeutic approach for liver cancer. Delivery of microRNAs in the liver is more efficient in comparison to other tissues, and a recent study revealed that delivery of the antisense-microRNA-122 suppressed hepatitis C viremia in primates, with no evidence of viral resistance or side effects (Lanford et al., 2010), leading to the initiation of phase I clinical trials in HCV-infected patients. This work lays the ground for testing whether miR-124 can also exert tumor-suppressive effects in human liver cancers. Together, our findings elucidate a molecular mechanism that is responsible for the initiation and maintenance of the hepatocyte-transformed phenotype, which enhances our understanding of liver cancer pathogenesis and provides a microRNA therapeutic strategy for prevention and treatment of liver cancer. Though we have identified a novel molecular circuit that is essential for the transformation of hepatocytes and is found to be perturbed in different HCC models and in human hepatocellular carcinomas, significant work remains to identify the driver signaling pathways involved in hepatocellular carcinogenesis.

EXPERIMENTAL PROCEDURES

Extensive details for all experimental procedures are provided in the Extended Experimental Procedures.

Cell Culture

Human nontransformed immortalized hepatocytes (IMH1, IMH2) were purchased from ATCC (cat no. CRL-4020) and from Xenotech LLC (cat. no. IFH15), respectively. Detailed description of the origin of these immortalized hepatocytes and their culture conditions can be found in the Extended Experimental Procedures. In addition, human liver cancer cell lines (HepG2, Hep3B, SNU-449, SNU-398, and SNU-387) were purchased from ATCC. Human liver cancer cell lines HepG2 and Hep3B were maintained in DMEM medium (GIBCO) supplemented with 10% FBS and 10 units/ml penicillin and 100 μg/ml streptomycin. SNU-449, SNU-398, and SNU-387 were maintained in RPMI-1640 medium (GIBCO) supplemented with 10% FBS and 10 units/ml penicillin and 100 μg/ml streptomycin.

MicroRNA Library HNF4α Screening

A microRNA library consisting of 317 microRNA mimics and two microRNA negative control mimics (100 nM) (Dharmacon Inc) was transfected in HepG2 cells plated in 96-well plates. At 24 hr posttransfection, the cells were transfected with a firefly luciferase vector harboring the 3′UTR of HNF4α for 24 hr, and the luciferase activity was measured using the Dual Luciferase Reporter Assay System (Promega, WI, USA). MicroRNAs that inhibited > 75% the luciferase activity of HNF4α were considered as positive hits. Detailed experimental description can be found in the Extended Experimental Procedures.

TUNEL Assay

Apoptosis was determined using the DeadEnd Fluorometric TUNEL System (G3250, Promega), as previously described (Polytarchou et al., 2008).

Real-Time PCR Analysis

RNA purified from IMH, HepG2, Hep3B, SNU-449, SNU-398, SNU-387, and SNU-475 cells under different transfection conditions with siRNAs or microRNAs was reverse transcribed to form cDNA, which was subjected to SYBR Green-based real-time PCR analysis. MicroRNA expression levels were tested using the Exiqon PCR Primer Sets, according to the manufacturer's instructions (Exiqon Inc, Denmark). Primer sequences can be found in the Extended Experimental Procedures.

Identification of Transcription Factor Sites in MicroRNA Regulatory Areas

The Lever and PhylCRM algorithms have been used to identify STAT3 and HNF4α binding motifs in an area 5 kb upstream and 2 kb downstream of microRNAs. A detailed description of this method has been included in the Extended Experimental Procedures.

Mouse Experiments

All of the experiments in xenografts and DEN-treated mice are described analytically in the Extended Experimental Procedures.

RNA Expression Studies from Patient Samples

RNAs from 45 hepatocellular carcinomas and 12 normal tissues were purchased from Biochain (Hayward, CA) and Origene (Rockville, MD). The expression levels of miR-24, IL6R, miR-124, and HNF4α were analyzed by real-time RT-PCR in all of the tissue described above. Each sample was run in triplicate, and the data represent the mean ± SD.

SUPPLEMENTAL INFORMATION

Supplemental Information includes Extended Experimental Procedures, seven figures, and two tables and can be found with this article online at doi:10.1016/j.cell.2011.10.043.

ACKNOWLEDGMENTS

This work was supported by DFCI CIA start-up funds to D.I. and research grants to M.K. from the National Institutes of Health (RO1-CA118165 and P42-ES0100337). We would like to thank the Nikon Imaging Center at Harvard Medical School for their help with light microscopy. Also, we would like to thank Hye-Jung Kim for her assistance with the flow cytometry analysis and Virgilio Garcia for his technical support.

Received: February 16, 2011
Revised: July 22, 2011
Accepted: October 11, 2011
Published: December 8, 2011

REFERENCES

Ahn, S.H., Shah, Y.M., Inoue, J., Morimura, K., Kim, I., Yim, S., Lambert, G., Kurotani, R., Nagashima, K., Gonzalez, F.J., and Inoue, Y. (2008). Hepatocyte nuclear factor 4alpha in the intestinal epithelial cells protects against inflammatory bowel disease. Inflamm. Bowel Dis. *14*, 908–920.

Barrett, J.C., Lee, J.C., Lees, C.W., Prescott, N.J., Anderson, C.A., Phillips, A., Wesley, E., Parnell, K., Zhang, H., Drummond, H., et al; UK IBD Genetics Consortium; Wellcome Trust Case Control Consortium 2. (2009). Genome-wide association study of ulcerative colitis identifies three new susceptibility loci, including the HNF4A region. Nat. Genet. *41*, 1330–1334.

Bromberg, J.F., Wrzeszczynska, M.H., Devgan, G., Zhao, Y., Pestell, R.G., Albanese, C., and Darnell, J.E., Jr. (1999). Stat3 as an oncogene. Cell *98*, 295–303.

Calvisi, D.F., Ladu, S., Gorden, A., Farina, M., Conner, E.A., Lee, J.S., Factor, V.M., and Thorgeirsson, S.S. (2006). Ubiquitous activation of Ras and Jak/Stat pathways in human HCC. Gastroenterology *130*, 1117–1128.

Cattin, A.L., Le Beyec, J., Barreau, F., Saint-Just, S., Houllier, A., Gonzalez, F.J., Robine, S., Pinçon-Raymond, M., Cardot, P., Lacasa, M., and Ribeiro, A. (2009). Hepatocyte nuclear factor 4alpha, a key factor for homeostasis, cell architecture, and barrier function of the adult intestinal epithelium. Mol. Cell. Biol. *29*, 6294–6308.

Chen, W.S., Manova, K., Weinstein, D.C., Duncan, S.A., Plump, A.S., Prezioso, V.R., Bachvarova, R.F., and Darnell, J.E., Jr. (1994). Disruption of the HNF-4 gene, expressed in visceral endoderm, leads to cell death in embryonic ectoderm and impaired gastrulation of mouse embryos. Genes Dev. *8*, 2466–2477.

Colletti, M., Cicchini, C., Conigliaro, A., Santangelo, L., Alonzi, T., Pasquini, E., Tripodi, M., and Amicone, L. (2009). Convergence of Wnt signaling on the HNF4alpha-driven transcription in controlling liver zonation. Gastroenterology *137*, 660–672.

Coussens, L.M., and Werb, Z. (2002). Inflammation and cancer. Nature *420*, 860–867.

Darsigny, M., Babeu, J.P., Seidman, E.G., Gendron, F.P., Levy, E., Carrier, J., Perreault, N., and Boudreau, F. (2010). Hepatocyte nuclear factor-4alpha promotes gut neoplasia in mice and protects against the production of reactive oxygen species. Cancer Res. *70*, 9423–9433.

El-Serag, H.B., and Rudolph, K.L. (2007). Hepatocellular carcinoma: epidemiology and molecular carcinogenesis. Gastroenterology *132*, 2557–2576.

Elmén, J., Lindow, M., Schütz, S., Lawrence, M., Petri, A., Obad, S., Lindholm, M., Hedtjärn, M., Hansen, H.F., Berger, U., et al. (2008). LNA-mediated microRNA silencing in non-human primates. Nature *452*, 896–899.

Esau, C., Davis, S., Murray, S.F., Yu, X.X., Pandey, S.K., Pear, M., Watts, L., Booten, S.L., Graham, M., McKay, R., et al. (2006). miR-122 regulation of lipid metabolism revealed by in vivo antisense targeting. Cell Metab. *3*, 87–98.

Fabbri, M., Bottoni, A., Shimizu, M., Spizzo, R., Nicoloso, M.S., Rossi, S., Barbarotto, E., Cimmino, A., Adair, B., Wojcik, S.E., et al. (2011). Association of a microRNA/TP53 feedback circuitry with pathogenesis and outcome of B-cell chronic lymphocytic leukemia. JAMA *305*, 59–67.

Furuta, M., Kozaki, K.I., Tanaka, S., Arii, S., Imoto, I., and Inazawa, J. (2010). miR-124 and miR-203 are epigenetically silenced tumor-suppressive microRNAs in hepatocellular carcinoma. Carcinogenesis *31*, 766–776.

Gerstein, M.B., Lu, Z.J., Van Nostrand, E.L., Cheng, C., Arshinoff, B.I., Liu, T., Yip, K.Y., Robilotto, R., Rechtsteiner, A., Ikegami, K., et al; modENCODE Consortium. (2010). Integrative analysis of the Caenorhabditis elegans genome by the modENCODE project. Science *330*, 1775–1787.

Grivennikov, S., Karin, E., Terzic, J., Mucida, D., Yu, G.Y., Vallabhapurapu, S., Scheller, J., Rose-John, S., Cheroutre, H., Eckmann, L., and Karin, M. (2009). IL-6 and Stat3 are required for survival of intestinal epithelial cells and development of colitis-associated cancer. Cancer Cell *15*, 103–113.

Gupta, R.K., and Kaestner, K.H. (2004). HNF-4alpha: from MODY to late-onset type 2 diabetes. Trends Mol. Med. *10*, 521–524.

He, G., Yu, G.Y., Temkin, V., Ogata, H., Kuntzen, C., Sakurai, T., Sieghart, W., Peck-Radosavljevic, M., Leffert, H.L., and Karin, M. (2010). Hepatocyte IKKbeta/NF-kappaB inhibits tumor promotion and progression by preventing oxidative stress-driven STAT3 activation. Cancer Cell *17*, 286–297.

Hedvat, M., Huszar, D., Herrmann, A., Gozgit, J.M., Schroeder, A., Sheehy, A., Buettner, R., Proia, D., Kowolik, C.M., Xin, H., et al. (2009). The JAK2 inhibitor AZD1480 potently blocks Stat3 signaling and oncogenesis in solid tumors. Cancer Cell *16*, 487–497.

Iliopoulos, D., Hirsch, H.A., and Struhl, K. (2009). An epigenetic switch involving NF-kappaB, Lin28, Let-7 MicroRNA, and IL6 links inflammation to cell transformation. Cell *139*, 693–706.

Iliopoulos, D., Jaeger, S.A., Hirsch, H.A., Bulyk, M.L., and Struhl, K. (2010). STAT3 activation of miR-21 and miR-181b-1 via PTEN and CYLD are part of the epigenetic switch linking inflammation to cancer. Mol. Cell *39*, 493–506.

Jiang, R., Tan, Z., Deng, L., Chen, Y., Xia, Y., Gao, Y., Wang, X., and Sun, B. (2011). 22 promotes human hepatocellular carcinoma by activation of STAT3 (IL: Hepatology), Epub ahead of print.

Kardassis, D., Tzameli, I., Hadzopoulou-Cladaras, M., Talianidis, I., and Zannis, V. (1997). Distal apolipoprotein C-III regulatory elements F to J act as a general modular enhancer for proximal promoters that contain hormone response elements. Synergism between hepatic nuclear factor-4 molecules bound to the proximal promoter and distal enhancer sites. Arterioscler. Thromb. Vasc. Biol. *17*, 222–232.

Kent, O.A., Chivukula, R.R., Mullendore, M., Wentzel, E.A., Feldmann, G., Lee, K.H., Liu, S., Leach, S.D., Maitra, A., and Mendell, J.T. (2010). Repression of the miR-143/145 cluster by oncogenic Ras initiates a tumor-promoting feed-forward pathway. Genes Dev. *24*, 2754–2759.

Kota, J., Chivukula, R.R., O'Donnell, K.A., Wentzel, E.A., Montgomery, C.L., Hwang, H.W., Chang, T.C., Vivekanandan, P., Torbenson, M., Clark, K.R., et al. (2009). Therapeutic microRNA delivery suppresses tumorigenesis in a murine liver cancer model. Cell *137*, 1005–1017.

Kyrmizi, I., Hatzis, P., Katrakili, N., Tronche, F., Gonzalez, F.J., and Talianidis, I. (2006). Plasticity and expanding complexity of the hepatic transcription factor network during liver development. Genes Dev. *20*, 2293–2305.

Ladias, J.A., Hadzopoulou-Cladaras, M., Kardassis, D., Cardot, P., Cheng, J., Zannis, V., and Cladaras, C. (1992). Transcriptional regulation of human apolipoprotein genes ApoB, ApoCIII, and ApoAII by members of the steroid hormone receptor superfamily HNF-4, ARP-1, EAR-2, and EAR-3. J. Biol. Chem. *267*, 15849–15860.

Lanford, R.E., Hildebrandt-Eriksen, E.S., Petri, A., Persson, R., Lindow, M., Munk, M.E., Kauppinen, S., and Ørum, H. (2010). Therapeutic silencing of microRNA-122 in primates with chronic hepatitis C virus infection. Science *327*, 198–201.

Lujambio, A., Ropero, S., Ballestar, E., Fraga, M.F., Cerrato, C., Setién, F., Casado, S., Suarez-Gauthier, A., Sanchez-Cespedes, M., Git, A., et al. (2007).

Genetic unmasking of an epigenetically silenced microRNA in human cancer cells. Cancer Res. *67*, 1424–1429.

Maeda, S., Kamata, H., Luo, J.L., Leffert, H., and Karin, M. (2005). IKKbeta couples hepatocyte death to cytokine-driven compensatory proliferation that promotes chemical hepatocarcinogenesis. Cell *121*, 977–990.

Marcil, V., Seidman, E., Sinnett, D., Boudreau, F., Gendron, F.P., Beaulieu, J.F., Ménard, D., Precourt, L.P., Amre, D., and Levy, E. (2010). Modification in oxidative stress, inflammation, and lipoprotein assembly in response to hepatocyte nuclear factor 4alpha knockdown in intestinal epithelial cells. J. Biol. Chem. *285*, 40448–40460.

Martinez, N.J., Ow, M.C., Barrasa, M.I., Hammell, M., Sequerra, R., Doucette-Stamm, L., Roth, F.P., Ambros, V.R., and Walhout, A.J. (2008). A C. elegans genome-scale microRNA network contains composite feedback motifs with high flux capacity. Genes Dev. *22*, 2535–2549.

Odom, D.T., Zizlsperger, N., Gordon, D.B., Bell, G.W., Rinaldi, N.J., Murray, H.L., Volkert, T.L., Schreiber, J., Rolfe, P.A., Gifford, D.K., et al. (2004). Control of pancreas and liver gene expression by HNF transcription factors. Science *303*, 1378–1381.

Park, E.J., Lee, J.H., Yu, G.Y., He, G., Ali, S.R., Holzer, R.G., Osterreicher, C.H., Takahashi, H., and Karin, M. (2010). Dietary and genetic obesity promote liver inflammation and tumorigenesis by enhancing IL-6 and TNF expression. Cell *140*, 197–208.

Parviz, F., Matullo, C., Garrison, W.D., Savatski, L., Adamson, J.W., Ning, G., Kaestner, K.H., Rossi, J.M., Zaret, K.S., and Duncan, S.A. (2003). Hepatocyte nuclear factor 4alpha controls the development of a hepatic epithelium and liver morphogenesis. Nat. Genet. *34*, 292–296.

Polytarchou, C., Pfau, R., Hatziapostolou, M., and Tsichlis, P.N. (2008). The JmjC domain histone demethylase Ndy1 regulates redox homeostasis and protects cells from oxidative stress. Mol. Cell. Biol. *28*, 7451–7464.

Ptashne, M. (2009). Binding reactions: epigenetic switches, signal transduction and cancer. Curr. Biol. *19*, R234–R241.

Rebouissou, S., Amessou, M., Couchy, G., Poussin, K., Imbeaud, S., Pilati, C., Izard, T., Balabaud, C., Bioulac-Sage, P., and Zucman-Rossi, J. (2009). Frequent in-frame somatic deletions activate gp130 in inflammatory hepatocellular tumours. Nature *457*, 200–204.

Tacke, R.S., Tosello-Trampont, A., Nguyen, V., Mullins, D.W., and Hahn, Y.S. (2011). Extracellular hepatitis C virus core protein activates STAT3 in human monocytes/macrophages/dendritic cells via an IL-6 autocrine pathway. J. Biol. Chem. *286*, 10847–10855.

Villanueva, A., Newell, P., Chiang, D.Y., Friedman, S.L., and Llovet, J.M. (2007). Genomics and signaling pathways in hepatocellular carcinoma. Semin. Liver Dis. *27*, 55–76.

Xu, L., Hui, L., Wang, S., Gong, J., Jin, Y., Wang, Y., Ji, Y., Wu, X., Han, Z., and Hu, G. (2001). Expression profiling suggested a regulatory role of liver-enriched transcription factors in human hepatocellular carcinoma. Cancer Res. *61*, 3176–3181.

Yin, C., Lin, Y., Zhang, X., Chen, Y.X., Zeng, X., Yue, H.Y., Hou, J.L., Deng, X., Zhang, J.P., Han, Z.G., and Xie, W.F. (2008). Differentiation therapy of hepatocellular carcinoma in mice with recombinant adenovirus carrying hepatocyte nuclear factor-4alpha gene. Hepatology *48*, 1528–1539.

Zhong, W., Sladek, F.M., and Darnell, J.E., Jr. (1993). The expression pattern of a Drosophila homolog to the mouse transcription factor HNF-4 suggests a determinative role in gut formation. EMBO J. *12*, 537–544.

Zhong, Z., Wen, Z., and Darnell, J.E., Jr. (1994). Stat3: a STAT family member activated by tyrosine phosphorylation in response to epidermal growth factor and interleukin-6. Science *264*, 95–98.

EXTENDED EXPERIMENTAL PROCEDURES

Cell Culture

Human non-transformed NeHepLxHT immortalized hepatocytes (IMH1) were purchased from ATCC (cat no. CRL-4020). This is a diploid human cell line of male origin which was developed from hepatocytes by transduction with a retroviral expression vector (pLXSN) containing the hTERT gene. IMH1 cells were maintained in DMEM:F12 medium supplemented with 10% heat-inactivated FBS, 0.1 μl/ ml dexamethasone from HMM Hepatocyte Medium SingleQuot (Lonza/ Clonetics Catalog # CC-4192), 0.11 μl/ ml insulin from HMM Hepatocyte Medium SingleQuot (Lonza/ Clonetics Catalog # CC-4192), 50ug/ml G-418 and 10 units/ml penicillin, and 100 μg/ml streptomycin.

The immortalized hepatocyte cell line (designated Fa2N-4) was purchased from Xenotech LLC (cat. no. IFH15). The cell line (IMH2) was isolated from normal human hepatocytes of female origin and transformed with the SV40 virus large T-antigen. Fa2N-4 hepatocytes attach to collagen (Purecol/MCDI solution, Purecol from Fisher Scientific cat no. 50-360-230/MCDI from Sigma C10640-2) and adopt the well-defined, cubical shape that is characteristic of human primary hepatocytes. The cells were thawed and plated using the Multi-Function Enhancing (MFE) Plating medium F (Xenotech LLC, cat no. K4005) supplemented with 5 units/ml penicillin, 50 μg/ml streptomycin, and 10% component B (Xenotech LLC). The MFE plating medium F was replaced with serum-free MFE Support medium F (Xenotech LLC, cat no. K4105), supplemented with 5 units/ml penicillin, and 50 μg/ml streptomycin, 4 hr after plating. The next day the medium was replaced by MFE Support medium F supplemented with MFE supplement A (Xenotech LLC) and the cells were subjected to the appropriate analysis.

Human liver cancer cell lines HepG2 were maintained in DMEM medium (GIBCO) supplemented with 10% FBS and 10 units/ml penicillin, and 100 μg/ml streptomycin. SNU-449 cells were maintained in RPMI-1640 medium (GIBCO) supplemented with 10% FBS and 10 units/ml penicillin, and 100 μg/ml streptomycin.

Reagents

SiRNAs: The following siRNAs were used in this study: siRNA negative control (siNC, cat no. AM4611, Ambion Inc) and two different siRNAs against HNF4α (siHNF4α#1, cat no. s6696, Ambion Inc) and (siHNF4α#2, cat no. s6698, Ambion Inc).

ShRNAs: shRNA control (pGFP-V-RS, cat. no TR30007, Origene Inc), shRNA against HNF4α (shHNF4α#1, cat.no TG320382, Origene Inc).

MicroRNAs: miR-24 (cat no. C-300497-03-0005, Dharmacon Inc), as-miR-24 (cat no. IH-300497-03-0005, Dharmacon Inc), miR-629 (cat no. C301129-01-0005, Dharmacon Inc), as-miR-629 (cat no. C301129-02-0005, Dharmacon Inc), miR-124 (cat no. C-300593-05-0005, Dharmacon Inc), as-miR-124 (cat no. IH-300593-06-005, Dharmacon Inc), miR NC (cat no. CN-001000-01-05, Dharmacon Inc) and as-miR NC (cat no. IN-001005-01-05, Dharmacon Inc).

Antibodies: HNF4α (sc-6556, Santa Cruz Biotech Inc), STAT3 (9139, Cell signaling), pSTAT3 (9138, Cell Signaling), IL6R (sc-13947, Santa Cruz Biotech Inc) and b-actin (4970, Santa Cruz Biotech Inc).

MicroRNA Library Screen

A microRNA library, consisting of 317 microRNA mimics and 2 microRNA negative control mimics (100nM) (Dharmacon Inc) was transfected in HepG2 cells plated in 96-well plates (three replicates). The transfection dose of 100nM for the microRNA mimics was detected through control experiments performed to identify the maximum dose without any cytotoxic effects. 24h post-transfection, the cells were transfected with a firefly luciferase vector harboring the 3′UTR of HNF4α (cat no. HmiT008908-MT01, Genecopoeia Inc) for 24h and the luciferase activity was measured using the Dual Luciferase Reporter Assay System (Promega, WI, USA). MicroRNAs that inhibited > 75% the luciferase activity of HNF4α in all three replicates were considered as positive hits. Comparison of the three replicates suggested high reproducibility of the screen. Furthermore, we performed a secondary screen using a 3′UTR vector that does not have any binding sites for the positive hits microRNAs identified from the primary screen, showing the specificity of our findings. The positive hits identified in the primary screen were validated in secondary screens in HepG2 and Hep3B cells (Figure 1C). Specifically 100nM of these microRNA mimics were transfected in HepG2 and Hep3B cells plated in 6-well plates, 24h post-transfection, HepG2 and Hep3B cells were transfected with the firefly luciferase vector harboring the 3′UTR of HNF4α for 24h and the luciferase activity was measured using the Dual Luciferase Reporter Assay System. The identification of these hits in both HepG2 and Hep3B cell lines, suggest that the findings of the primary screen are not cell line-dependent.

Colony Formation Assay

IMH1, IMH2, HepG2, Hep3B, and SNU-449 cells were transfected with shRNAs, siRNAs or microRNAs for 48h. Then, triplicate samples of 10^5 cells from each cell line were mixed 4:1 (v/v) with 2.0% agarose in growth medium for a final concentration of 0.4% agarose. The cell mixture was plated on top of a solidified layer of 0.8% agarose in growth medium. Cells were fed every 6 to 7 days with growth medium containing 0.4% agarose. The number of colonies was counted after 20 days. The experiment was repeated thrice and the statistical significance was calculated using Student's t test.

Invasion Assays

We performed invasion assays in IMH1, IMH2, HepG2, Hep3B and SNU-449 cells under different transfection conditions with siRNAs or microRNAs for 24h. Invasion of matrigel has been conducted by using standardized conditions with BDBioCoat growth factor reduced MATRIGEL invasion chambers (PharMingen). Assays were conducted according to manufacturer's protocol, by using 10% FBS as chemoattractant. Non-invading cells on the top side of the membrane were removed while invading cells were fixed and stained with 4′-6-diamidino-2-phenylindole (DAPI, Vector Laboratories Inc.), 16h post seeding. In all assays, 10 fields per insert were scored and SD was measured. The experiment was repeated thrice and the statistical significance was calculated using Student's t test.

Real-Time PCR Analysis

RNA purified from IMH1, IMH2, HepG2, Hep3B and SNU-449 cells under different transfection conditions with siRNAs or microRNAs was reverse-transcribed to form cDNA, which was subjected to SYBR Green based real-time PCR analysis. Primers used for actin forward: 5′-CCTGTACGCCAACACAGTGC-3′ and reverse 5′-ATACTCCTG CTTGCTGATCC-3′; HNF4α forward: 5′-TGTCCCGACA GATCACCTC-3′ and reverse 5′-CACTCAACGAGAACCAGCAG-3′; ApoCIII forward: 5′-GGGTACTCCTTGTTGTTGC-3′ and reverse: 5′-AAATCCCAGAA CTCAGAGAAC-3′; ALDOB forward: 5′-AGGAGGACTCTTCTCTCCCAA-3′ and reverse: 5′-GATTCATCTG CAGCCAGGAT-3′; CYP1A2 forward: 5′-CTGGCCTCTG CCATCTTCTG-3′ and reverse: 5′-TTAGCCTCCTTGCTCACATGC-3′; CYP7A1 forward: 5′- CAGTGCCTCCCTCAACATCC-3′ and reverse: 5′-GACATATTGTAGCTCCC GATCC-3′; PEPCK forward: 5′-AGCTCGGTCGCTGGATGTCAGAG-3′ and reverse 5′-GTAGGGTGAATCCGTCAGCTCGATG-3′; G6P forward: 5′-GGCTCCAT GACTGTGGGATC-3′ and reverse: 5′-TTCAGCTGCACAGCCCAGAA-3′; IL6R forward: 5′-TGCCAGTATTCCCAGGAGTC-3′ and reverse: 5′-GGCAGTGACTGTGATGTTGG-3′.

MicroRNA Real-Time PCR Analysis

MicroRNA expression levels were tested using the Exiqon PCR Primer Sets, according to the manufacturer's instructions (Exiqon Inc, Denmark). Specifically we tested the expression levels of miR-24 (cat no. 204260, Exiqon), miR-629 (cat no. 204370) and miR-124 (cat no. 204319). U6 expression was used as an internal control. The expression levels of these microRNAs in liver cancer cell lines were normalized to the microRNA levels of the immortalized hepatocytes (IMH1). The experiments have been performed in triplicate and data are presented as mean ± SD.

Western Blot Analysis

Protein samples were subjected to SDS PAGE and transferred to polyvinylidene difluoride membranes in 25 mM Tris, 192 mM glycine. Membranes were blocked with 5% nonfat dry milk in PBS, 0.05% Tween-20 and probed with antibodies (1:1000) followed by corresponding horseradish peroxidase-labeled secondary antibodies (1:1000). Blots were developed with ECL reagent (PerkinElmer Life Sciences, Waltham, MA) and exposed in Eastman Kodak Co. 440 Image Station.

Cell Cycle Analysis

Cells were trypsinized, pelleted at 1,000 x g and 4°C for 5 min, and lysed in lysis-staining buffer (3.4 mM sodium citrate, 10 mM NaCl, 0.1% Nonidet P-40, 75 μM ethidium bromide [EtBr]) (1 ml/10^6 cells on ice). The fluorescence intensity of cell nuclei was measured by fluorescence-activated cell sorter (FACS) analysis.

BrdU Staining

DNA synthesis was determined using the 5-Bromo-2′-deoxy-Uridine (BrdU) Labeling and Detection Kit II according to manufacturer's instructions (11299964001, Roche).

Caspase Luciferase Activity

Relative 3/7 caspase activity was measured using the Caspase-Glo 3/7 Assay according to manufacturer's instructions (G8091, Promega). Measurements were normalized to the respective cell numbers which were determined using the CellTiter-Glo Luminescent Cell Viability Assay (G7571, Promega). Results are expressed as the percent of the ratio of caspase activity/cell number compared to the siControl-treated cells (Figure S18).

Bio-Plex Phospho-STAT3 ELISA Assay

This sandwich ELISA assay (cat. no 171-V22552, Bio-rad) assessed the phosphorylation status of tyrosine 705 of STAT3 protein in ELISA in HepG2, Hep3B and SNU-449 cells treated 100nM siRNA NC, siRNA against HNF4α (siHNF4α#1), miR-24 and/or miR-629, as-miR-NC, as-miR-124 for 24h. The data were analyzed in a Bio-plex FlexMap3D analyzer using the Bio-plex manager software.

Cleaved Caspase-3 ELISA Assay

PathScan Cleaved Caspase-3 (Asp175) Sandwich ELISA Kit is a solid phase sandwich enzyme-linked immunosorbent assay (ELISA) that detects endogenous levels of cleaved caspase-3 protein (Cell Signaling Inc, cat no. 7190). A total Caspase-3 Antibody has been coated onto the microwells. After incubation with cell lysates, the caspase-3 (cleaved and uncleaved) protein is captured by the coated antibody. Following extensive washing, A biotinylated Cleaved Caspase-3 Antibody is added to detect the captured cleaved caspase-3 protein. HRP-linked streptavidin is then used to recognize the bound detection antibody. HRP substrate, TMB, is added to develop color. The magnitude of optical density for this developed color is proportional to the quantity of cleaved caspase-3 protein.

This assay was used to measure the levels of cleaved caspase-3 in DEN-treated mice which were administered with miR-NC or miR-124 (data presented in Figure 6D).

Cleaved PARP ELISA Assay

PathScan Cleaved PARP (Asp214) Sandwich ELISA Kit is a solid phase sandwich enzyme-linked immunosorbent assay (ELISA) that detects endogenous levels of cleaved PARP (Asp214) protein (Cell Signaling Inc, cat no. 7262). A cleaved PARP (Asp214) Mouse mAb* has been coated onto the microwells. After incubation with cell lysates, cleaved PARP (Asp214) protein is captured by the coated antibody. Following extensive washing, PARP Rabbit mAb is added to detect the captured cleaved PARP protein. Anti-rabbit IgG, HRP-linked Antibody is then used to recognize the bound detection antibody. HRP substrate, TMB, is added to develop color. The magnitude of the absorbance for this developed color is proportional to the quantity of cleaved PARP (Asp214) protein. This assay was used to measure the levels of cleaved PARP in DEN-treated mice which were administered with miR-NC or miR-124 (data presented in Figure 6D).

IL6 ELISA Assay

This assay (R&D Systems, cat. no D6050) Systems employs the quantitative sandwich enzyme immunoassay technique. A monoclonal antibody specific for IL-6 has been pre-coated onto a microplate. Standards and samples are pipetted into the wells and any IL-6 present is bound by the immobilized antibody. After washing away any unbound substances, an enzyme-linked polyclonal antibody, for IL-6 is added to the wells. Following a wash to remove any unbound antibody-enzyme reagent, a substrate solution is added to the wells and color develops in proportion to the amount of IL-6 bound in the initial step. The color development is stopped and the intensity of the color is measured.

IL6R ELISA Assay

The Sino Biological ELISA kit (cat no. SEK10398) is a solid phase sandwich ELISA (Enzyme-Linked Immunosorbent Assay). It utilizes a monoclonal antibody specific for IL6R coated on a 96-well plate. Standards and samples are added to the wells, and any IL6R present binds to the immobilized antibody. The wells are washed and a biotinylated rabbit anti-IL6R polyclonal antibody is then added, producing an antibody-antigen-antibody "sandwich." To produces color in proportion to the amount of IL6R / CD126 present in the sample streptavidin-HRP and TMB substrate solution are loaded. The absorbances of the microwell are read at 450 nm.

Both IL6 and IL6R assays were used to measure soluble IL6R levels in untreated, 1nM of siRNA NC or 1nM of siRNA against HNF4a (siHNF4a#1) in HepG2, Hep3B and SNU-449 cells, 24h post transfection (data are shown in figure S16A, B). Furthermore, we measured IL6R levels soluble in IMH1 cells transfected with 1nM siRNA NC or siHNF4a#1, using this assay (data shown in figure S17H). In addition, we measured IL6 and IL6R levels in human hepatocellular tissues (data shown in Figure 7E).

Serum Assays

Aspartate aminotransferase (AST), alanine aminotransferase (ALT), total bilirubin and urea levels in mice were determined with commercially available kits (Sigma).

Luciferase Assays

Untreated or miR-NC, miR-124, as-miR NC, as-miR-124 (100nM) treated HepG2 cells were transfected with a firefly luciferase reporter gene construct containing the 3′UTR of IL6R (HmiT009672-MT01, Genecopoeia Inc) Cell extracts were prepared 24h after transfection of the luciferase vector, and the luciferase activity was measured using the Dual Luciferase Reporter Assay System (Promega, WI, USA). In addition, HepG2 cells were transfected with a firefly luciferase reporter gene construct containing the miR-124 regulatory area (wild-type or deletion mutant in the HNF4α binding site) and 12 and 24h post treatment with IL6 (20ng/ml) were lysed and the luciferase activity was measured using the Dual Luciferase Reporter Assay System (Promega, WI, USA).

MicroRNA Target Prediction Analysis

The miRNA database TargetScan version 5.1 (http://www.targetscan.org/index.html) was used to identify potential miR-124, miR-24 and miR-629 targets.

Identification of Transcription Factor Sites in MicroRNA Regulatory Areas

The Lever and PhylCRM algorithms were developed previously and are described in a separate paper (Warner, J. et al. Systematic identification of mammalian regulatory motifs' target genes and their functions (Warner et al., 2008). In order to identify STAT3 and HNF4α binding motifs in an area of 5kb upstream and 2kb downstream of microRNAs we used three selection criteria: 1) First we examined the presence of STAT3 and HNF4α binding motifs using Lever algorithm. Lever assesses whether the motifs are enriched in *cis*-regulatory modules (CRMs), in the noncoding sequences surrounding the genes; 2) For the identified binding sites we incorporated phylogenetic information from 12 different mammal species (mouse, rat, human, rabbit, chimp, macaque, cow, dog, armadillo, tenrec, opossum and elephant) and selected only the binding sites with high conservation scores (a conserved motif is considered one with a score higher than 100) by using PhylCRM algorithm (for more details see Warner et al., 2008). 3) Then, we mapped the conserved binding sites in the regions of interest, as well as visually inspecting the nucleosome occupancy in the conserved binding sites shown as part of the UCSC genome browser track.

STAT3 binding sites: The predicted and conserved STAT3 binding motif in miR-24 was located in chromosome 19:13,808,863-13,808,870 and had a conservation score of 198.97, the predicted and conserved STAT3 binding motif in miR-629 was located in chromosome 15: 68,176,873-68,176,880 and had a conservation score of 159.72.

HNF4α binding sites: The chromosomal coordinates and conservation scores for the predicted HNF4α binding sites in microRNA regulatory areas are shown in Table S1.

Chromatin Immunoprecipitation

Chromatin immunoprecipitation was carried out as described previously (Iliopoulos et al., 2010). Briefly, the chromatin fragments, derived from untreated and IL6-treated (6, 12, 24h) SNU-449 cells, were immunoprecipitated with 6ug of antibody against STAT3. DNA extraction was performed using QIAGEN Purification Kit. Real-time PCR analysis was performed for STAT3 binding sites in microRNA regulatory areas using the following primers: miR-24: forward 5′-ATGGGGAGAGGAAGCCAAG-3′ and reverse 5′-CTAAGCCCTGGCCACTGA-3′ (PCR product: 150bp); miR-629: forward 5′-CCCCCTCGGAGAGGAGAG-3′ and reverse 5′-GTGCCCGCTGGACTTAGG-3′ (PCR product: 150). In addition, chromatin immunoprecipitation was performed in HepG2 and SNU-449 cells by using 9 μg of antibody against HNF4α. Real-time PCR analysis was performed for HNF4 binding sites in microRNA regulatory areas using the following primers: miR-7-1: forward 5′- TTGATTTACAATGCGGCAAA-3′ and reverse 5′- TCCCCTTTA GACGGTGTATTG-3′ (PCR product: 169bp); miR-124: forward 5′-AGAGGAAGAGACCGGGAGTG-3′ and reverse 5′- TTGA GAAGCCCTG GACAGAT-3′ (PCR product: 152bp).

Mouse Experiments

$5x10^6$ IMH1 cells transfected with 100nM siRNA NC or siHNF4α#1 or siHNF4α#2 or microRNA negative control (miR NC) or miR-24 and/or miR-629 for 48h were injected subcutaneously in the right flank of NOD-SCID mice (five mice/group). Tumor growth was monitored every five days for a total period of 30-55 days. Tumor volumes were calculated by the equation $V(mm^3) = axb^2/2$, where a is the largest diameter and b is the perpendicular diameter. In addition, $5x10^6$ SNU-449 cells were injected subcutaneously in the right flank of NOD-SCID mice. On days 15, 20 and 25 the mice were injected (10mg/kg) intraperitoneously with: i) microRNA negative control (miR-NC); ii) antisense-microRNA negative control (as-miR NC); iii) miR-24 and/or miR-629; iv) as-miR-24 and/or as-miR-629; v) miR-24 and miR-629 (five mice/group). Tumor volume was monitored for 55 days.

Also, male mice on a C57BL/6 background were maintained in filter-topped cages and were fed standard rodent chow and water ad libitum. To induce hepatocellular carcinogenesis, mice were injected intraperitoneally (i.p.) with 25mg/kg of diethylnitrosamine (DEN) (Sigma) at 15 days of age. The mice were observed for development of tumors every 4 weeks and tumors were identified 32 weeks (~8 months) post DEN treatment. At weeks 1, 4, 8, 12, 24 and 32 mice (5 mice/group) were sacrificed and liver tissues were collected. Ricin A chain was used to eliminate Kupffer cells and endothelial cells and purify hepatocytes (Johnston and Jasuja, 1994). HNF4α and IL6R mRNA expression levels and miR-124 and miR-24 levels were assessed by real-time PCR analysis in the purified hepatocytes.

Therapeutic Protocol

15 male C57BL/6 mice were DEN-treated and 32 weeks post treatment they were randomly distributed into 3 groups. The first group of mice did not receive any treatment, the second group of mice was treated with 10mg/kg microRNA-negative control (miR-NC) and the third group of mice was treated with 10mg/kg miR-124 (Exiqon Inc). MiR-NC and miR-124 were encapsulated in liposomes (In-vivofectamine 2.0, Invitrogen) prior to injections. These liposomes have been designed for systemic microRNA delivery with high in vivo transfection efficiency in the liver following tail vein injection. Briefly, Invivofectamine 2.0 reagent is mixed with the microRNA and they are incubated for 30 min at 50°C. MicroRNAs in a volume of 200ul were injected in the tail vein of the mice. MicroRNA treatments were performed in a weekly basis (week 33, 34, 35). At week 36, mice were sacrificed and tumor burden was assessed. Externally visible tumors larger than 0.5mm were counted using stereo microscopy. Primary hepatocytes were purified as described above and RNA and protein were extracted. MiR-124 levels, HNF4α and IL6R mRNA levels were assessed by real-time PCR analysis, while STAT3 and phosphorylated STAT3 (Tyr705) status were assessed by Western blot analysis.

Prevention Protocol

15 male C57BL/6 mice were DEN-treated and 12 weeks post treatment they were randomly distributed into 3 groups. The first group of mice did not receive any treatment, the second group of mice was treated with 10mg/kg microRNA-negative control (miR-NC) and the third group of mice was treated with 10mg/kg miR-124. MicroRNAs were encapsulated in liposomes as described above and treatments were performed biweekly (weeks 12, 14, 16, 18, 20, 22, 24, 26, 28, 30). At week 32, mice were sacrificed and tumor burden was assessed as described above. Primary hepatocytes were purified from mouse liver tissues, RNA was extracted and miR-124 expression levels were assessed by real-time PCR analysis (Ambion Inc).

Hepatocyte Conditional Knockout Mouse Experiment

$STAT3^{f/f}$ and $STAT3^{\Delta hep}$ male mice were treated with 25 kg/mg DEN when 15 days old. Mice were sacrificed 8 months later and tumor tissues from DEN-treated $STAT3^{\Delta hep}$ mice and DEN-treated $STAT3^{f/f}$ mice were collected (same tumors as the ones described in Figures 6B, C of He et al., 2010). From 4 tumors derived from the $STAT3^{\Delta hep}$ mice and 4 tumors from $STAT3^{f/f}$ mice, we extracted RNA and tested the expression levels of HNF4α, miR-124, miR-24 and miR-629. The mouse experiments have been performed in accordance with the University of California San Diego (UCSD) and Dana-Farber Cancer Institute Animal Care Committee guidelines.

Patient Samples

RNA samples: RNAs from 45 hepatocellular carcinomas and 12 normal tissues were purchased from Biochain (Hayward, CA) and Origene (Rockville, MD). The expression levels of miR-24, IL6R, miR-124 and HNF4α were analyzed by real-time RT-PCR in all the tissues described above. Each sample was run in triplicate and the data represent the mean ± SD.

Tissue samples: FFPE samples from 8 normal liver and 31 hepatocellular carcinomas were provided by Stanford University School of Medicine. An informed consent has been obtained from all subjects and the study has been approved by the Institutional Review Board of Stanford University. Hepatocytes were captured by laser capture microdissection and RNA (RNeasy FFPE Kit, cat no. 73504, QIAGEN Inc) and protein (QProteome FFPE Tissue Kit, cat no. 37623, QIAGEN Inc) were extracted. All the samples were negative for CD45 expression, validating the absence of immune cells in these samples. RNA was used to perform real-time PCR analysis for HNF4a, miR-124, IL6R, miR-24 and miR-629 and protein was used to perform ELISA analysis for IL6, IL6R and phosphorylated STAT3.

In Situ MicroRNA Hybridization

Double-DIG labeled Mircury LNA probes for the detection of hsa-miR-24 (18121-15, Exiqon), hsa-miR-124 (88066-15, Exiqon) and hsa-miR-629 (38699-15, Exiqon) by in situ hybridization, were used as previously described (Iliopoulos et al., 2009) with modifications. FFPE sections of normal liver and HCCs were deparaffinized with xylene (3x5 min), followed by treatment with serial dilutions of ethanol (3x100%, 2x96% and 3x70%) and by two changes of DEPC-PBS. Tissues were then digested with proteinase K (15 μg/ml) for 20 min at 37°C, rinsed with 3xDEPC-PBS. Sections were dehydrated with 2x70%, 2x96% and 2x100% ethanol, air-dried and hybridized for 1 hr with the hsa-miR-24, hsa-miR-124 or hsa-miR-629 probe (40 nM) or the double-DIG labeled U6 Control Probe (1 nM) (99002-15, Exiqon) diluted in microRNA ISH buffer (90000, Exiqon), at 60, 60, 55 and 53°C, respectively. Following hybridization, sections were rinsed twice with 5XSSC, 2x1XSSC and 3x0.2XSSC, 5 min each, at the hybridization temperatures and PBS. The slides were incubated with blocking solution (11585762001, Roche) for 15 min and then with anti-DIG antibody (1:800) in 2% sheep serum (013-000-121, Jackson Immunoresearch) blocking solution for 1 hr, at RT. Following three washes with PBS-T (PBS, 0.1% Tween-20), slides were incubated with the AP substrate buffer (NBT-BCIP tablet [11697471001, Roche] in 10 ml of 0.2 mM Levamisole [31742, Fluka]) for 2 hr at 30°C in the dark. The reaction was stopped with 2 washes of AP stop solution (50 mM Tris-HCl, 150 mM NaCl, 10 mM KCl) and 2 washes with water. Tissues were counter stained with Nuclear Fast Red for 1 min and rinsed with water. Sections were dehydrated with 2x70%, 2x96% and 2x100% ethanol and mounted with coverslips in Eukitt mounting medium (361894G, VWR). Images were captured with a Nikon 80i Upright Microscope equipped with a Nikon Digital Sight DS-Fi1 color camera, using the NIS-Elements image acquisition software. All images were captured and processed using identical settings.

Immunohistochemistry

For tissue immunostaining for HNF4α and phospho-STAT3, FFPE sections of normal liver and HCCs were deparaffinized with xylene (3x5 min) followed by treatment with serial dilutions of ethanol (100%, 100%, 95% and 95%, 10 min each) and by two changes of ddH_2O. Antigen unmasking was achieved by boiling the slides (95-99°C) for 10 min, in 10 mM sodium citrate (for HNF4α), pH 6.0, or 1 mM EDTA pH 8.0 (for phospho-STAT3). Sections were rinsed three times with ddH_2O, immersed in 3% H_2O_2 for 20 min, washed twice with ddH_2O and once with TBS-T (TBS, 0.1% Tween-20) and blocked for 1 hr with blocking solution (5% normal goat serum [5425] in TBS-T). HNF4A (3113, Cell Signaling Technology) and phospho-STAT3 (Tyr705) (9145, Cell Signaling Technology) antibodies were diluted 1:50 in Signal Stain antibody diluent (8112, Cell Signaling Technology) and incubated with the sections overnight at 4°C. Following incubation with the antibodies, sections were washed three times, 5 min each, with TBS-T and incubated for 1 hr at room temperature with SignalStain Boost ([HRP, Rabbit] 8114, Cell Signaling Technology). Sections were washed three times, 5 min each, with TBS-T, and stained with the DAB Peroxidase Substrate Kit (SK-4100, Vector Laboratories) for 30 min, washed and counterstained with the hematoxylin QS (H-3404, Vector Laboratories). Finally, tissues were dehydrated and mounted in Eukitt medium. Images were captured with a Nikon 80i Upright Microscope equipped with a Nikon Digital Sight DS-Fi1 color camera, using the NIS-Elements image acquisition software. All images were captured and processed using identical settings in the Nikon Imaging Center at Harvard Medical School.

SUPPLEMENTAL REFERENCES

Iliopoulos, D., Polytarchou, C., Hatziapostolou, M., Kottakis, F., Maroulakou, I.G., Struhl, K., and Tsichlis, P.N. (2009b). MicroRNAs differentially regulated by Akt isoforms control EMT and stem cell renewal in cancer cells. Sci. Signal. *2*, ra62.

Johnston, D.E., and Jasuja, R. (1994). Purification of cultured primary rat hepatocytes using selection with ricin A subunit. Hepatology *20*, 436–444.

Warner, J.B., Philippakis, A.A., Jaeger, S.A., He, F.S., Lin, J., and Bulyk, M.L. (2008). Systematic identification of mammalian regulatory motifs' target genes and functions. Nat. Methods *5*, 347–353.

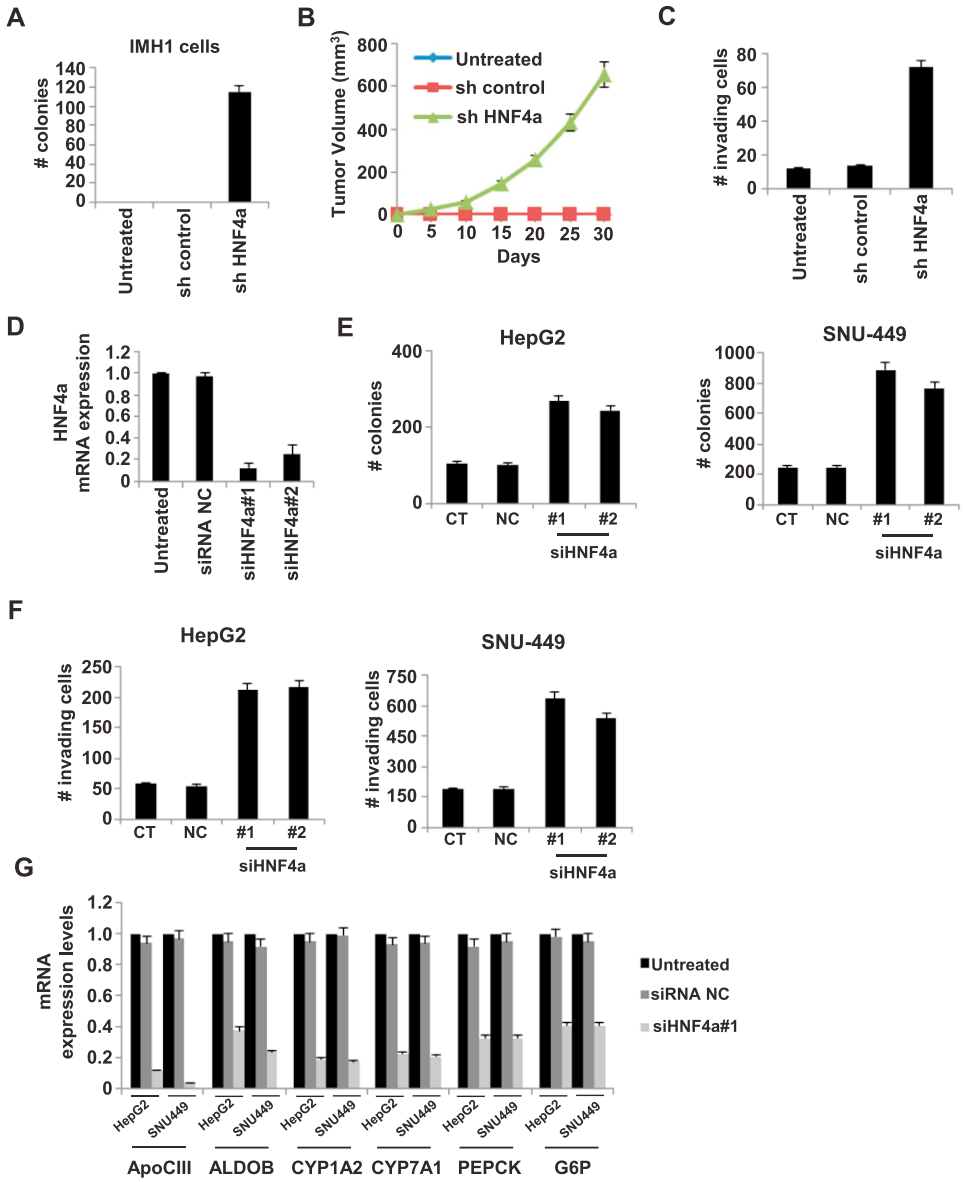

Figure S1. HNF4α Suppression Induces Hepatocellular Transformation, Related to Figure 1

(A) Soft-agar colony assay of non transformed immortalized hepatocytes (IMH1) treated with shRNA empty vector (sh control) or shRNA against HNF4α (sh HNF4α). Colonies 50 μm were counted using a microscope 20 days later. The mean together with SD of a representative experiment done in triplicate is shown.

(B) Tumor volume (mean ± SD) in mice injected with untreated or treated with sh control or shHNF4α IMH1 cells. Tumor volume was monitored 30 days post injection.

(C) Invasion assay of non transformed immortalized hepatocytes (IMH1) treated with shRNA empty vector (sh control) or shRNA against HNF4α (sh HNF4α).

(D) HNF4α expression levels in xenograft tumors. HNF4α mRNA expression assessed by real-time RT-PCR analysis in tumors (55 days) derived from injected IMH1 cells that were untreated or treated for 48h with 1nM siRNA negative control (siRNA NC) or two different siRNAs against HNF4α (siHNF4α#1, siHNF4α#2).

(E and F) (E) Soft agar colony assay and (F) invasion assays in HepG2 and SNU-449 hepatocellular cancer cell lines untreated (CT) or treated for 48h with siRNA negative control (NC) and two siRNAs against HNF4α. The experiments have been performed in triplicate and the data show mean ± SD.

(G) Expression levels of HNF4α direct downstream targets in liver cells. ApoCIII, ALDOB, CYP1A2, CYP7A1 and GP6 mRNA levels were assessed by real-time RT-PCR analysis in HepG2 and SNU449 cells untreated or treated with 1nM siRNA negative control (siRNA NC) or siRNA against HNF4α (siHNF4α#1).

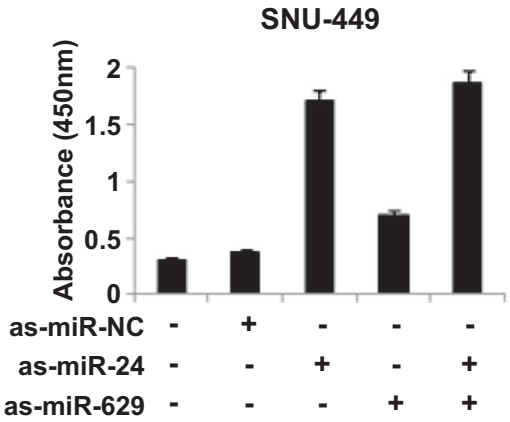

Figure S2. Suppression of miR-24 and miR-629 Induces Apoptosis in HCC Xenograft Tumors, Related to Figure 2

The levels of cleaved caspase-3 activity were measured by ELISA assay in the same tumors, described in Figure 2G. The data suggest that inhibition of miR-24 and/or miR-629 by antisense-microRNAs leads to decreased tumor growth due to induction of apoptosis.

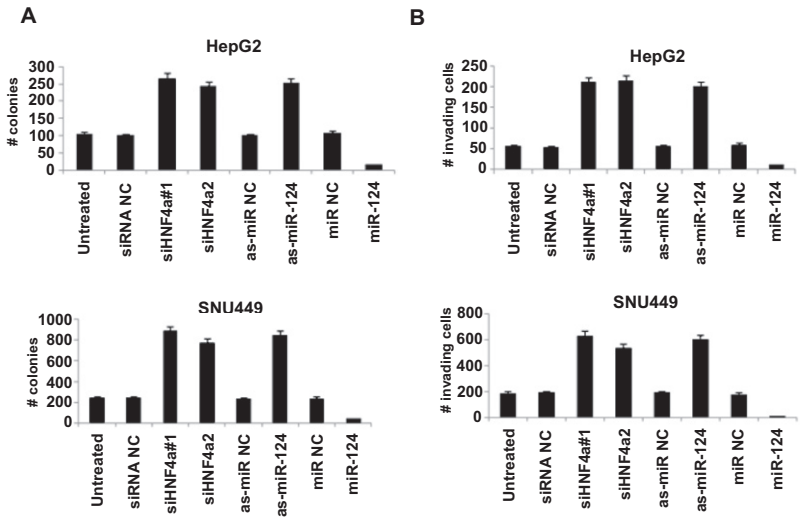

Figure S3. Inhibition of miR-124 Expression Has Similar Effects with HNF4α Inhibition in the Colony Formation and Invasive Ability of Hepatocellular Cancer Cells, Related to Figure 4

(A and B) (A) Soft agar colony assay and (B) invasion assays in HepG2 and SNU-449 hepatocellular cancer cell lines untreated or treated for 24h with siRNA negative control (siRNA NC) and two siRNAs against HNF4α or antisense-microRNA negative control (as-miR-NC), antisense-microRNA-124 (as-miR-124), microRNA negative control (miR NC) and microRNA-124 (miR-124). The experiments have been performed in triplicate and the data show mean ± SD.

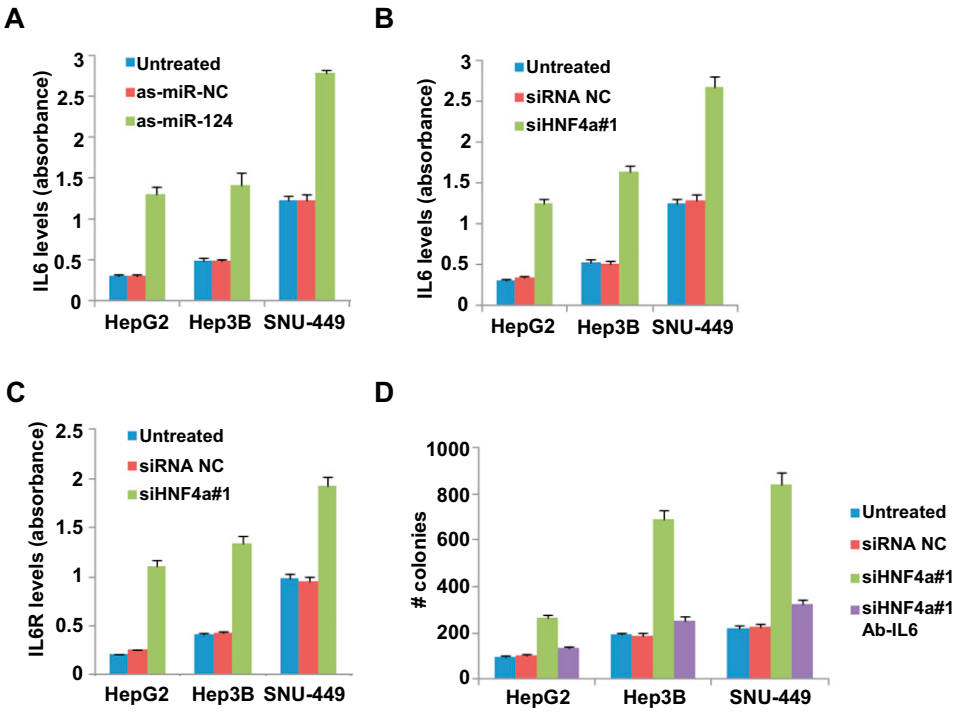

Figure S4. HNF4a Circuit Regulates the Production of IL6 and IL6R in Liver Cancer Cells, Related to Figure 4

(A) Soluble IL6 levels were measured in untreated, as-miR-NC or as-miR-124 treated HepG2, Hep3B and SNU-449 cells, 24h post transfection by ELISA assay. (B and C) (B) Soluble IL6 and (C) IL6R levels were measured in untreated, 1nM of siRNA NC or 1nM of siRNA against HNF4a (siHNF4a#1) in HepG2, Hep3B and SNU-449 cells, 24h post transfection by ELISA assay. The data are presented as mean ± SD of three independent experiments and show that inhibition of HNF4a expression increases the levels of soluble IL6 and IL6R in liver cancer cells, suggesting that perturbation of the HNF4a circuit drives liver cancer cells to an activated inflammatory state.

(D) Soft-agar colony assay in HepG2, Hep3B and SNU-449 cells treated for 24h with 1nM siRNA NC or siHNF4a#1 or siHNF4a#1 followed by Ab-IL6 for 24h. The data are presented as mean ± SD of three independent experiments.

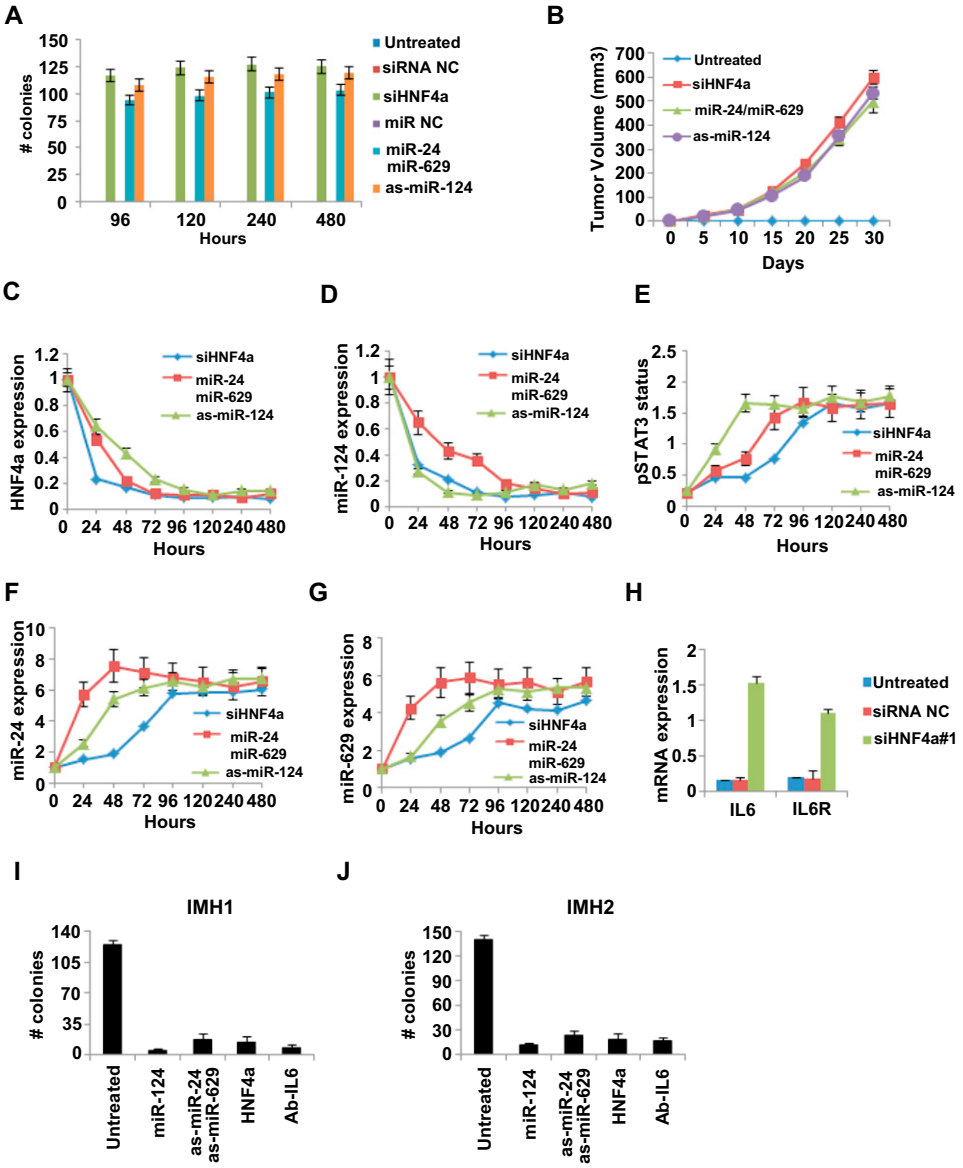

Figure S5. The HNF4α Feedback Loop Circuit Is Perturbed during Hepatocellular Transformation In Vitro and In Vivo, Related to Figure 4

(A) Soft-agar colony assay of IMH cells transiently transfected with the respective miRNAs or siRNAs for 24h. These cells were maintained in culture 96-480h post-transfection and then were plated in soft agar and colony number was assessed 20 days later.

(B) Tumor volume (mean ± SD) in mice injected with IMH cells untreated or treated with siHNF4α, miR-24 and miR-629, as-miR-124 for 24h and then maintained in culture for 120h before being injected in nude mice.

(C–G) Assessment of HNF4α, miR-124, miR-24, miR-629 levels by real-time RT-PCR analysis and of STAT3 phosphorylation levels by ELISA in IMH1 cells transiently transfected with 1nM siHNF4α or miR-24 and miR-629 or as-miR-124.

(H) Assessment of soluble IL6 and IL6R by ELISA assay in IMH1 cells, 96h after transfection with 1nM siRNA NC or siHNF4a#1.

(I) Assessment of colony formation in soft agar of IMH1 cells and (J) IMH2 cells untreated or treated with 100nM miR-124 or as-miR-24 and as-miR-629 or HNF4α for 48h. These cells were propagated for 20 days (480h) post treatments and then were plated in soft agar and their colony formation ability was tested 20 days later.

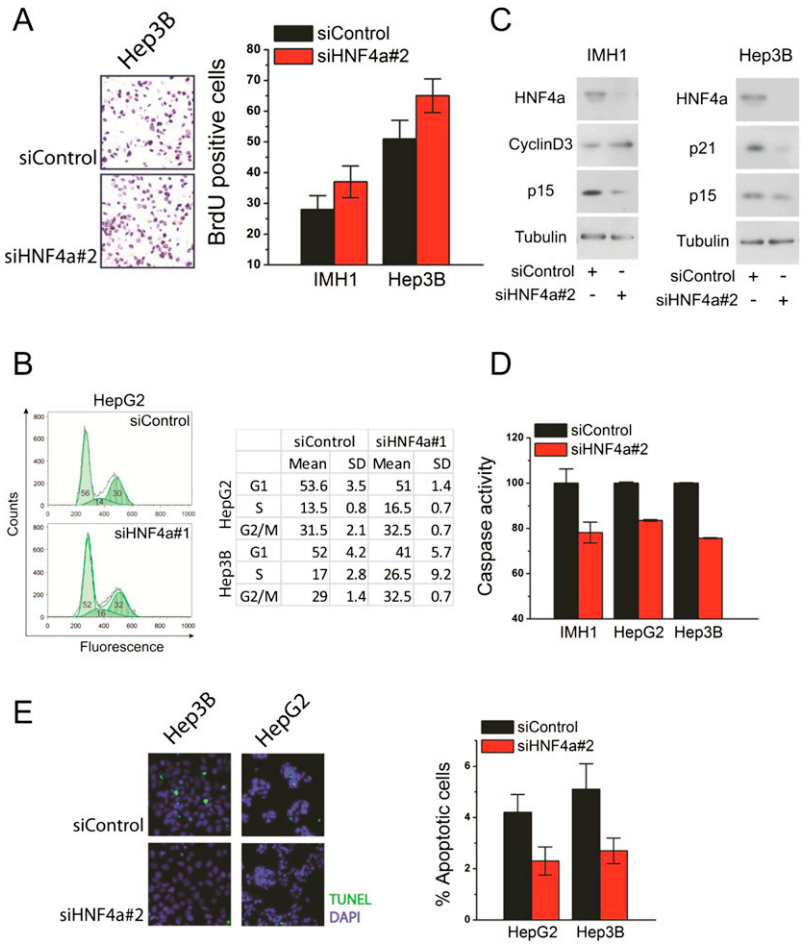

		siControl		siHNF4a#1	
		Mean	SD	Mean	SD
HepG2	G1	53.6	3.5	51	1.4
	S	13.5	0.8	16.5	0.7
	G2/M	31.5	2.1	32.5	0.7
Hep3B	G1	52	4.2	41	5.7
	S	17	2.8	26.5	9.2
	G2/M	29	1.4	32.5	0.7

Figure S6. Knockdown of HNF4α Induces Cell Growth and Renders Cells Resistant to Apoptosis, Related to Figure 4

(A) Cell proliferation as determined by the BrdU assay. Cells were transfected with siHNF4α or with siRNA NC and 48 hr later cell proliferation was determined using the BrdU assay. Data are mean percentages of BrdU positive cells ± SEM.

(B) Cell cycle analysis. The DNA contents of cells harvested 48 hr after HNF4α knockdown were determined. (Left) Representative plots of FACS analysis in HepG2 cells transfected with siControl (upper panel) and si HNF4α (lower panel). (Right) The percentages of cells in the G1, S, and G2/M phases of the cell cycle were measured and the mean percentage of cells in a given phase ± the SEM is derived from three independent experiments.

(C) Lysates of cells were harvested 48 hr after the transfection and analyzed by Western blotting for the detection of cell cycle regulation proteins. Tubulin was used as the loading control.

(D) Cells were transfected with siHNF4α or with siControl and 48 hr later caspase3/7 activity was determined. Data are mean percentages of caspase3/7 activity ± SEM.

(E) Apoptosis was determined by the TUNEL assay. 48 hr after transfection of the cells with the indicated siRNAs tunel staining was performed and the samples were examined by fluorescence microscopy. Data are expressed as the mean percentages of apoptotic cells ± SEM.

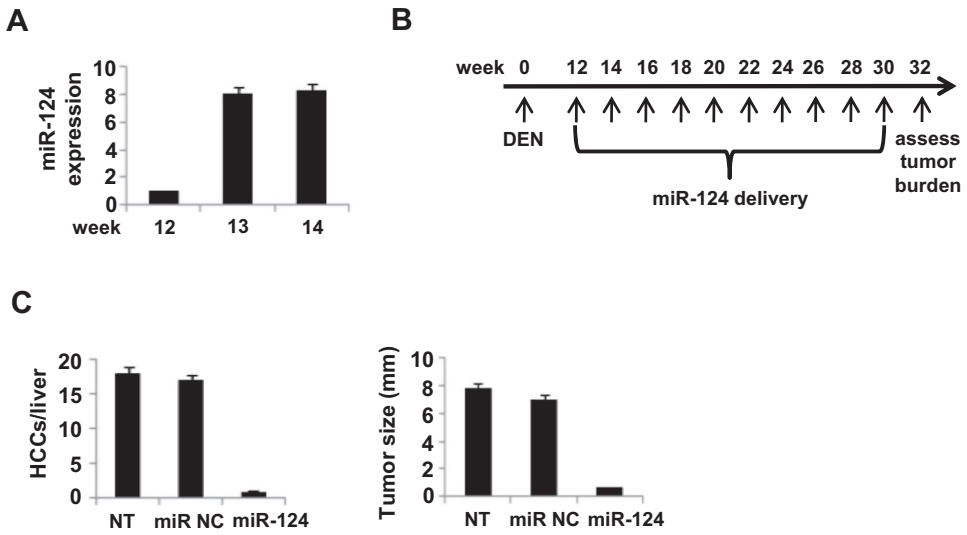

Figure S7. Preventive Effects of miR-124 Administration in Hepatocellular Oncogenesis, Related to Figure 6

(A) Assessment of miR-124 levels (mean ± SD) in liver tissues derived from DEN-treated mice (weeks 12, 13, 14) after systemic delivery of miR-124 on the first day of week 12.

(B) Timeline of miR-124 prevention delivery experiment.

(C) Number of tumors/liver and tumor size (mm^3) in non-treated (NT), miR-NC and miR-124 treated mice (week 32).